CONDITION ASSESSMENT OF KEVLAR COMPOSITE MATERIALS USING RAMAN SPECTROSCOPY

A Thesis presented to the Faculty of the Graduate School of the

University of Missouri – Columbia

In Partial Fulfillment of the Requirements for the Degree

Master of Science

By

THOMAS MICHAEL BRINTEN BROOKS II

Dr. Glenn Washer, Graduate Advisor

MAY 2007

The undersigned, appointed by the dean of the Graduate School, have examined the thesis entitled

CONDITION ASSESSMENT OF KEVLAR COMPOSITE MATERIALS USING RAMAN SPECTROSCOPY

Presented by Thomas Michael Brinten Brooks II,

A candidate for the degree of Master of Science,

And hereby certify that, in their opinion, it is worthy of acceptance.

Professor Glenn Washer

Professor V.S. Gopalaratnam

Professor Steven Neal

ACKNOWLEDGEMENTS

I would like to express my sincere gratitude to my advisor and friend, Dr. Glenn Washer, Assistant Professor of the Department of Civil and Environmental Engineering at the University of Missouri-Columbia. Dr. Washer's guidance and confidence in my abilities have been invaluable to me while studying under his direction.

I would also like to thank Dr. Steve Martin, Professor of the Department of Materials Science and Engineering at Iowa State University. His technical expertise and assistance with the testing apparatus was critical to my research and development. Also I would like to offer my appreciation to his graduate students who assisted me with any problems that arose with my tests.

Finally gratitude is extended to Scott Thorton, Shawn Arnett and Tom Yolken of Texas Research International (TRI), Austin, Texas, for supplying the materials used in this study, and for technical assistance and support.

TABLE OF CONTENTS

LIST OF FIGURES

LIST OF TABLES

ABSTRACT

This thesis presents the results of an investigation of the Raman scattering effects of aging Kevlar composite strands. The goal of this research is to investigate the potential application of Raman spectroscopy as a nondestructive evaluation tool for the detection of aging effects of in-service composite materials. Kevlar composites used as over-wrapping of metal-lined composite over-wrapped pressure vessels (COPVs) have been analyzed. Raman spectra produced from the Kevlar fibers and the effects of resin materials, utilized to bind the fibers into strands to provide composite behavior, have been investigated. A series of Kevlar / epoxy strands exposed to elevated temperatures and sustained loading have been evaluated. It was found that this exposure had an effect on the width and intensity of certain bands in the Raman spectra of Kevlar. The potential application of these findings to the nondestructive evaluation of Kevlar composites is discussed.

1

INTRODUCTION

1.1. Goal

There are concerns about the long-term behavior of polymer materials such as Kevlar that can be susceptible to aging effects, environmental degradation and stress rupture. Stress rupture is of particular concern in applications such as composite over-wrapped pressure vessels (COPVs), where a fiber/matrix composite over-wraps a metallic liner and acts as the primary load-bearing material when the vessel is pressurized. As a result, the composite material may be maintained at elevated stress levels for extended periods of time. Pressure vessel designs that include composite over-wrapping are preferred for space vehicles because of their low weight relative to all-metal vessels. Tanks of this design are utilized for various NASA vehicles, and there are concerns that aging effects and stress rupture could affect the performance characteristics of these vessels. To mitigate the risks associated with aging materials, nondestructive evaluation (NDE) technologies that can detect the onset of materials degradation are needed. The overall goal of the research reported here was to evaluate Raman

spectroscopy as a potential NDE tool for the detection of aging effects in composite materials, particularly the phenomena of stress rupture.

There have been many studies that have examined the application of Raman spectroscopy for the characterization of polymer materials such as Kevlar [1]. The relationship of Raman peaks with the vibrational characteristics of the polymer material provides insight on the interatomic bonding and elastic stresses within the molecules themselves.

Polymer materials such as Kevlar suffer from stress rupture: a loss in residual material strength that results from long-term exposure to increased stress. Stress rupture is a temperature-sensitive failure mode in which small increases in temperature for an extended period of time can greatly reduce the stress rupture lifetime of the material. The mechanisms leading to this loss of strength are not well understood. For practical engineering applications, where Kevlar fibers may be used as reinforcement in composite materials, there is a need to determine the effects of aging on the load carrying capacity of the fibers, particularly to determine when a material is nearing the end of its useful life. However, to date there have been no methods or techniques developed that can quantify the effective “age” of the material in-situ, toward the goal of predicting the onset of stress rupture. Instead, reliability models must be depended on to predict when stress rupture is likely to effect a material, based on the loading and temperature history. For polymer materials such as Kevlar, stress rupture has considerable variation using reliability models [2]. Temperature and loading history data is also frequently unavailable, making the prediction of the onset of stress rupture highly uncertain for most cases. It would therefore be advantageous to develop a method or technology that could detect the onset

of stress rupture by direct measurement or characterization of the material. Raman spectroscopy may be a solution to detect precursors to the stress rupture phenomenon based on the vibrational characteristics of polymer materials.

The relationship of Raman scattered light with the vibrational characteristics of molecules has potential to provide insight into the materials aging, i.e. loss of residual strength through molecular changes of the Kevlar fibers. This study explored the empirical relationships between the Raman band characteristics and the effects of aging Kevlar materials by a combination of elevated stress and temperatures. The initial objective of the research was to develop and understand the Raman spectrum of Kevlar materials to provide a foundation for the development of NDE technologies based on the interaction of scattered laser light with the polymer. The fundamental aspects of experimental characterization of the spectrum of Kevlar, and the effects of the environmental degradation of Kevlar materials on certain characteristics of its Raman spectrum are discussed.

It is hypothesized that the reduction in residual material strength associated with stress rupture phenomena may manifest from changes or damage in the polymer at a molecular level that may effect the vibrational characteristics of the material. Consequently the Raman spectra produced from the material may be affected. If the changes to the vibrational spectra of the material could be related to exposure to elevated temperatures and stress, and the reduction in residual strength which leads to stress rupture, the technique may have the potential to detect the onset of stress rupture in materials in-situ. This may provide a tool for the nondestructive evaluation of engineered components and structures.

1.2. Approach/Thesis

The approach of this project is to evaluate the empirical relationship between the intensity, band width and proximate wavenumber of a series of Raman peaks (bands) from Kevlar in an effort to identify trends that can be correlated with stress rupture phenomena. The objective for this portion of the study was to test a series of Kevlar strand samples that had been aged under various conditions and evaluate differences and trends in the Raman response to predict the onset of stress rupture. The effects of using different wavelength incident lasers were also evaluated along with other experimental parameters in an effort to understand the wavelength with the greatest potential for development. With these correct testing parameters, a firm foundation was set for further evaluation of the spectra for stress rupture detection in Kevlar fiber/matrix composites.

Although degradation modes for fiber reinforced polymers (FRPs) have been identified, NDE methods to detect the onset of these phenomena have yet to be developed. The focus of NDE development for composite materials has been mechanical damage and/or debonding between composite layers and substrate [3]. Detection of loss of fiber mechanical properties over time has remained largely unexplored, and significant gaps exist in the full understanding of the durability of FRP materials [4]. For example, precursors to stress rupture have not been identified, and there is currently no known nondestructive evaluation (NDE) method that can predict the onset of this phenomenon. In fact, there are presently no NDE methods developed that attempt to learn the condition of the fiber materials in FRPs independent of bulk composite properties, which are frequently dominated by the matrix. Initial efforts were first performed to explore Raman

spectroscopy as a potential NDE method for condition assessment of FRP material. As will be discussed, the Raman spectra of certain composite fibers relates to the vibrational properties of fiber molecules. As a result, the Raman spectra of the material are dependant on crystal and polymer structures, applied strain, and other factors. Changes in intensity, band width and proximate wavenumber may occur in the spectra due to the change in vibrational properties of the material. Therefore, this technique may have applications such as detecting fiber strains effected by loss of matrix/fiber bonding, loss of load sharing properties, and deterioration of the fiber itself.

This study reports on exploratory efforts to identify and understand the Raman spectra of Kevlar composite strands, compare the identified spectra results with the literature, and develop trends in the spectra that will predict the onset of stress rupture in Kevlar fiber reinforced composites.

2

BACKGROUND

2.1. Kevlar Composites

The use of polymer composite materials for the design and construction of engineered components has increased steadily since Kevlar was first introduced by the Du Pont de Nemours Inc. in 1971. Kevlar-fiber reinforced composite material is a strong, lightweight material consisting of Kevlar fibers embedded in a matrix sometimes called a fiber reinforced polymer (FRP). Kevlar fibers are organic fibers made from a polymer material. These fibers consist of long molecular chains produced from a synthetic polyamide in which the amide linkages are attached directly between two aromatic rings. For the case of Kevlar, an amide linkage is a carbonyl group (C=O) single bonded to a nitrogen atom, and an aromatic ring consists of six carbon atoms connected by alternating single and double covalent bonds. Figure 2-1 illustrates the polymer structure of Kevlar. From the figure, the Kevlar polymer structure is illustrated. The molecular long chains of Kevlar are highly oriented with many interchain hydrogen bonds and aromatic stacking interaction resulting in high energy absorption.

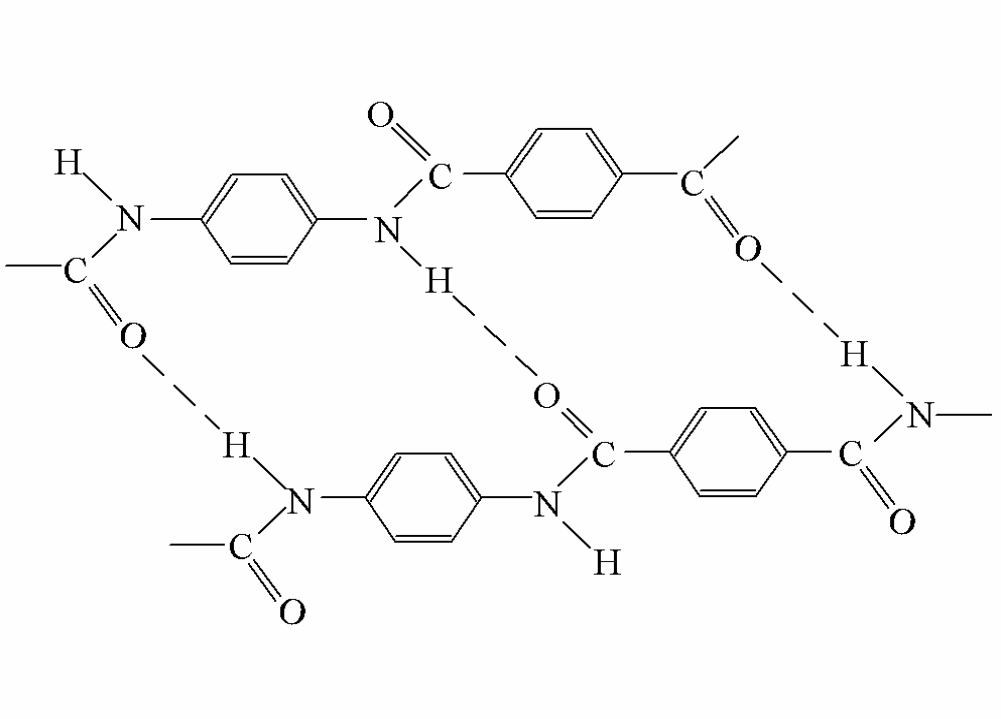

Figure 2-1. Chemical structure of Kevlar.

The advantages of Kevlar fiber include high tensile strength-to-weight ratio and modulus-to-weight ratio, low density, corrosion resistance and high design flexibility. These properties make Kevlar fibers ideal for engineering composites. These fibers have a much higher tensile modulus than steel wire, fiberglass, nylon and polyester fibers. Kevlar fibers have an elastic modulus from 550 to 1,100 GPa depending on filament yarn type. These fibers also have a low elongation break (2.8% for Kevlar 49), which is comparable to steel. Kevlar fibers have a low compressive strength and the mechanical properties vary with temperature. The thermal resistance of Kevlar ranges from -251 to 160 °C [5]. The material is also susceptible to creep, absorbs moisture, and is sensitive to

ultraviolet light. Generally, fiber creep increases with increasing stress and temperature. Kevlar fiber creep also increases with the presence of water.

Kevlar fibers are embedded in a matrix resin to form a composite section. The most commonly used matrix resin is a slow-setting epoxy. This type of resin requires a long process time which includes gelling for 4-16 hours and curing for 2-3 hours [5]. These epoxy impregnated strands have an elastic modulus of ~525 GPa and an elongation break of 2.9% for Kevlar 49. The strength of a fiber-reinforced composite can be controlled by the reinforcing fiber and the matrix resin on a volume basis.

2.2. Degradation of Kevlar Composites

There are concerns about the long-term performance of Kevlar composite materials which can be effected by harsh environmental conditions. For example, polymer materials are known to be damaged by exposure to ultraviolet (UV) radiation due to alterations in the chemical structure of the polymer that occur. Kevlar, glass and to a lesser extent carbon materials can also be effected by stress rupture, also known as creep rupture; a reduction in strength that occurs due to a combination of temperature, time and applied stress. It is also known that composite materials can be effected by a loss of mechanical bonding between the matrix material and the fibers. This results in a loss of the composite behavior that gives the material its strength and durability. Water absorption by the matrix material can cause expansion of the matrix, microcracking and a loss of strength. Extreme temperatures may also cause residual strains due to differences in thermal expansion between the fiber and matrix.

A study was conducted to test the environmental damage of composite sections [6]. The experimenters found that cyclic UV radiation and condensation lead to extensive matrix erosion, matrix microcracking, fiber debonding, fiber loss and void formation. The UV photons absorbed by the polymer composite materials result in photo-oxidative reactions that cause molecular chain scission and/or chain crosslinking. These photo-oxidative reactions occur when the polymer loses electrons due to exposure to UV light. Chain scission is simply random bond breakages in the chemical structure, and this lowers the molecular weight of the polymer which reduces strength and heat resistance [6]. Chain cross-linking occurs when the covalent bonds that link together polymer chains are broken down leading to an increase in brittleness of polymer structure and could result in microcracking of the fibers. Therefore, this composite degradation leads to inefficient fiber to matrix load transfer creating elevated loads for individual fibers. Once a fiber fails, the loading sheds to adjacent fibers giving those fibers an increase in loading. This could lead to catastrophic failure due to multiple fiber failures. For the case of composite over-wrapped pressure vessels, which are expected to operate at a high pressure, such failure could result in loss of life.

2.3. Stress Rupture

Composite materials are generally affected by the phenomenon known as stress rupture, variously referred to as static fatigue, creep rupture or stress life rupture. The term is used to describe a loss in residual strength of composite materials resulting from sustained loading. As a result of this loss of residual strength, a composite material maintained at a constant load significantly less than its tensile capacity may fail suddenly.

The stress rupture life of a composite is the minimum time period that a composite maintains its structural integrity, considering the combined effects of stress, time at stress level, and its environment. In the case of Kevlar 49 material stress rupture has considerable variation [2]. The stress rupture failure of composite materials is understood mainly on a phenomenological level and as a result must be stochastically treated through probability models [7, 8]. The process has high thermal sensitivity, such that minor variations in ambient temperature can have a significant effect of the stress rupture lifetime. The combined effects of other environment variables (i.e. exposure to ultraviolet light, moisture, radiation, etc) are complex and not well understood.

The random nature of the phenomena results in wide variation in the median stress lifetime for materials of apparently the same composite/matrix combinations [9]. The large variations in lifetime distributions result in significant uncertainty in determining the anticipated lifetime and reliability of a particular system or component. Therefore, it would be advantageous to develop a measurement technology that could identify precursors to stress rupture failure, such that in-service materials that are at-risk could be identified and the risks of stress rupture failure mitigated.

The physical, morphological changes that occur leading to stress rupture include the fracture of individual fibers, presumably where some defects or flaws exists in the as-manufactured fibers, or develop as a result of applied stresses. The load carried by the individual fibers is transferred to surrounding fibers through the matrix of the composite, leading to overloading of adjacent fibers to form clusters. These clusters combine to reach a critical size in which fractures propagate, leading to the catastrophic failure of the entire composite [9].

2.4. Raman Spectroscopy

When an incident photon interacts with a molecule, the photon can be absorbed, reflected or scattered. Scattering can be elastic Rayleigh scattering or inelastic Raman scattering. Raman spectroscopy is the measurement of the intensity and frequency of this inelastically scattered light. The frequency is directly related to energy by the equation:

$E = h\upsilon$

Where:

E = energy of the photon (m^2 kg / s^2)

h = Planck's constant (6.626068×10^{-34} m^2 kg / s)

υ = frequency of the photon (Hz)

For the Rayleigh scattering process, the energy of the incident photon is unchanged. As for Raman scattering, the energy of the photon is shifted from the incident energy due to change from the vibrational energy of the molecule. Figure 2-2 demonstrates the Raman scattering of a single photon.

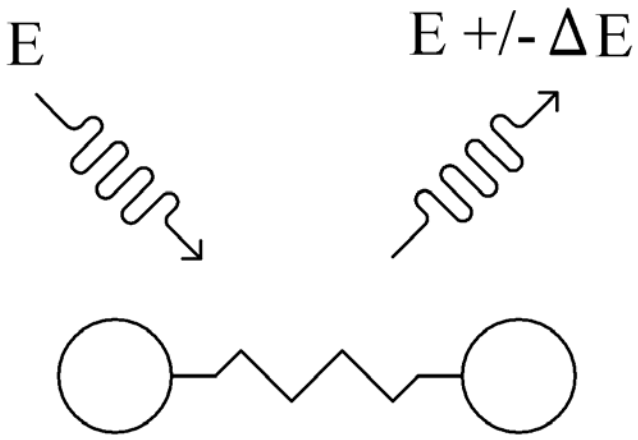

Figure 2-2. Energy of an incident photon interacts with a diatomic molecule and scatters the photon at a different Energy. This process is known as Raman scattering.

As a result of this shift in energy, the photon loses energy (Stokes scattering) and therefore the molecule that the light is incident upon has a higher vibrational energy. The photon can also gain energy (anti-Stokes scattering) and therefore create a downward shift in vibrational energy in the molecule. Stokes scattering is typically at higher intensities when compared to anti-Stokes scattering, as such Stokes scattering is typically evaluated to obtain Raman spectra. Figure 2-3 illustrates how a Raman spectrum is developed from Stokes scattering.

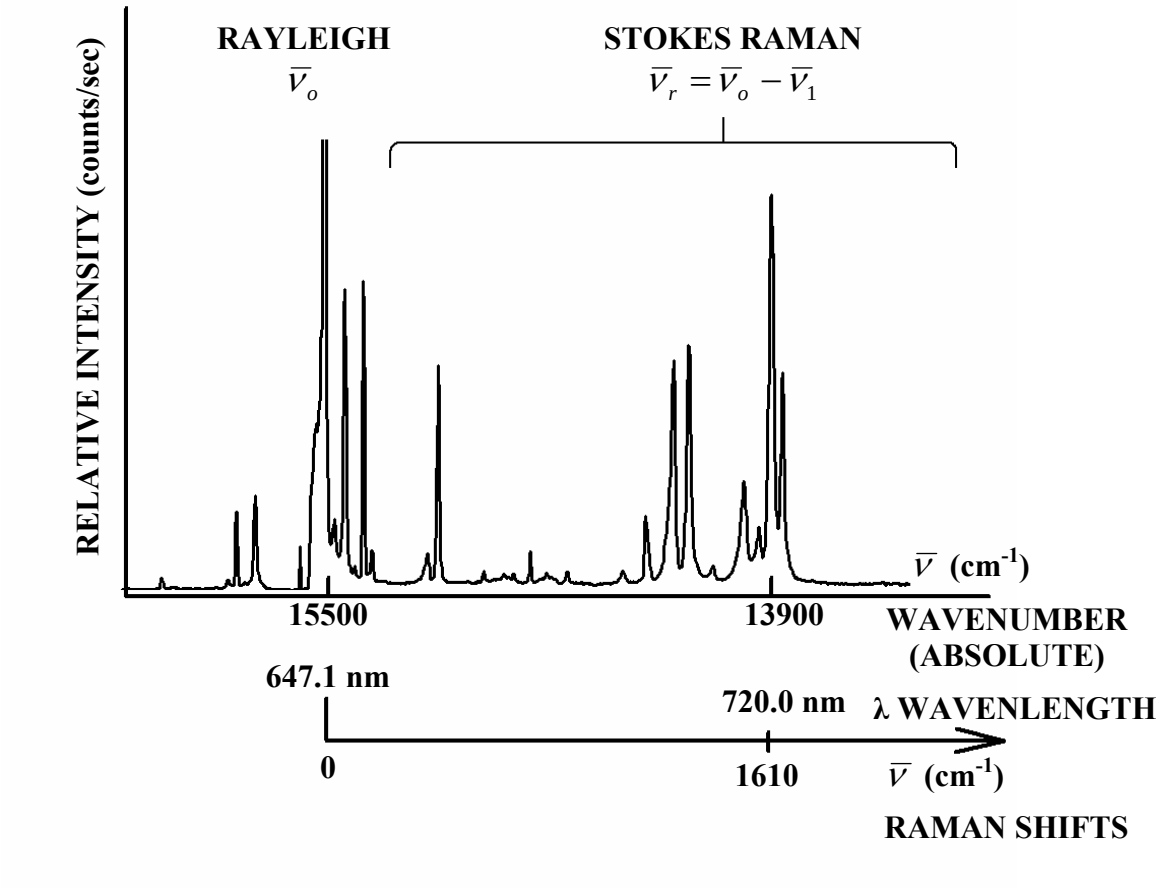

Figure 2-3. Raman spectrum of Kevlar illustrating the wavenumber conversion process.

From the figure, the abscissa is the absolute wavenumber of the scattered light and the relative wavenumber for the frequency shift from the incident laser light. The wavenumber is simply the inverse of the wavelength. The ordinate represents the relative intensity of the scattered photons per second, typically detected by a charge coupled device (CCD) or photomultiplier tube.

Raman spectra represent the frequency shift of the vibrational energy of the photon from the incident photon. These frequencies are converted into wavenumbers for the spectra. As shown in the figure, the absolute wavenumber of inelastic scattered light, $\bar{\nu}_1$, is subtracted from the absolute wavenumber of incident light, $\bar{\nu}_o$, to calculate a relative wavenumber to the incident light, $\bar{\nu}_r$. Therefore, the Stokes scattering equation becomes $\bar{\nu}_r = \bar{\nu}_o - \bar{\nu}_1$. The frequency shifts are dependent upon the specific molecular geometry of the material, and are independent of the incident photon frequency. For frequency shifts to occur, i.e. be Raman active, the polarizability of the molecule must change during vibration. The change in polarizability is considered the distortion of the expanding or contracting electron cloud surrounding the atomic cores to polarize the molecule. The polarization of the molecule is dependent upon the symmetry of the molecular vibration for a specific scattering geometry [10]. Therefore, a certain material could have many shifts in frequency from the incident photon, revealing a Raman spectrum. There are a number of peaks in the spectra of the polymer Kevlar, each that relate to a vibrational mode of the material.

When applying Raman spectroscopy to crystalline materials, the structure can be considered a set of harmonic oscillators with a spring constant between them. If no stress is applied to the molecule, the frequency of vibration is proportional to the square root of the spring constant. When the molecule is stressed, the Raman scattered light from the vibrational frequencies shifts to a different wavenumber due to the change in spring constant. Therefore, if the spring constants are known and the frequencies are measured, the external force can be determined [1]. Frequency shifts have not only been found in Kevlar, but carbon fibers as well [11]. The shift in frequency is dependent upon strain in

the fiber. Changes in the Raman band width and intensity may also occur when the Kevlar is strained.

To produce a Raman spectrum, a focused, monochromatic laser light is incident upon a sample and light is back scattered at 180° into a collection lens. Generally, the range of wavelengths of an incident laser is from 488 to 1064 nm for rigid chain polymer analyses. The inelastically scattered light is then guided through a monochromator and dispersed onto a CCD. The CCD is an optical-array detector which is advantageous due to its low readout noise. For a Raman spectrometer system, this process is shown on a schematic diagram (Figure 2-4). The Raman signal is then converted to an electrical signal by a CCD and stored on a PC. The Raman signal is converted to a wavenumber and subtracted from the wavenumber of the incident beam. The wavenumber of the incident laser is set to zero, and the Raman band assignments are relative to the zero mark to create a Raman spectrum.

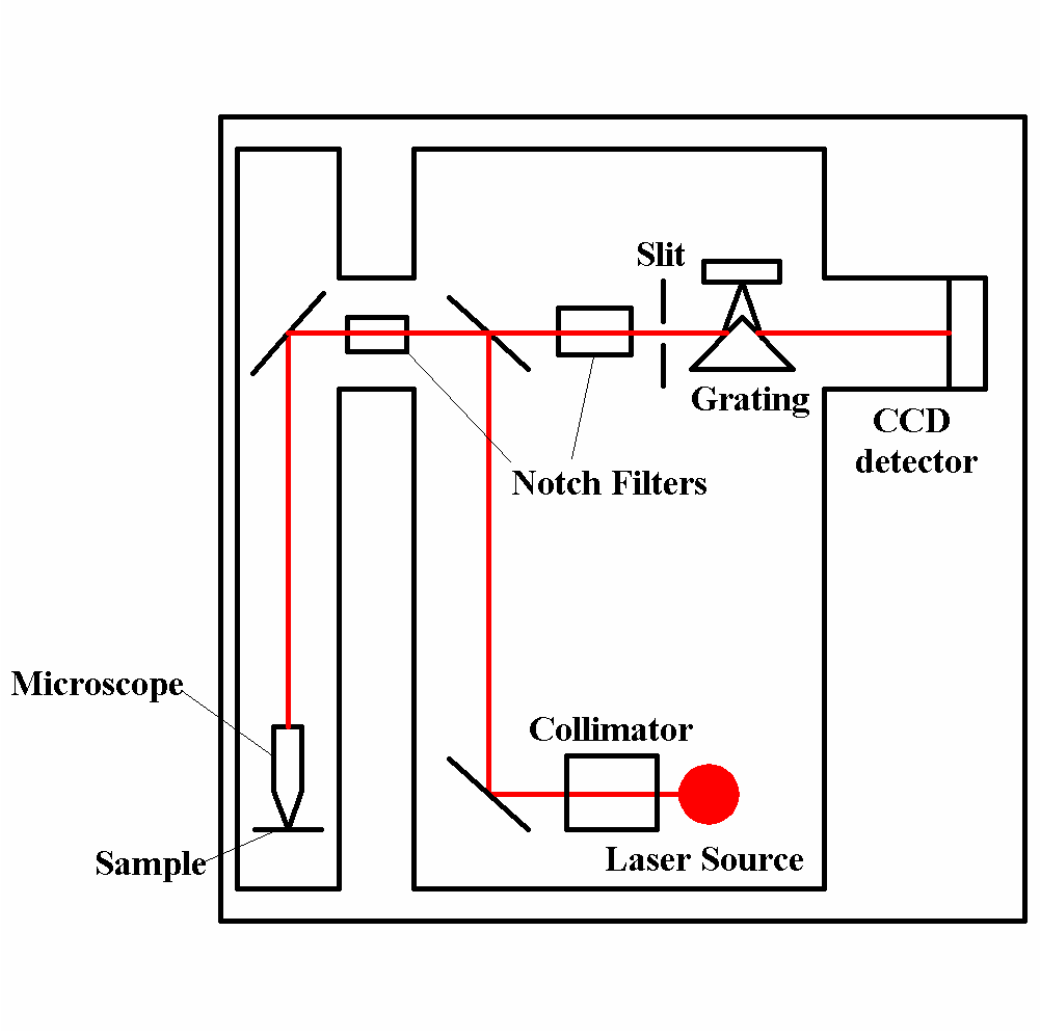

Figure 2-4. Schematic diagram of a Renishaw Raman spectrometer system.

2.5. Applications of Raman Spectroscopy

A Raman spectrum of Kevlar has very distinctive peaks due to its Raman scattering ability as shown in Figure 2-5. From the figure, two peaks are circled indicating the associated vibrational mode of the Kevlar monomer. For example, the 1613 cm^{-1} peak corresponds to the stretching of the C-C of the phenyl ring while the 1651 cm^{-1} peak corresponds to the C=O stretching of the Amide I linkage. Polymers have a C-C "backbone" which is highly coupled, therefore creating very strong Raman bands [10]. Raman scattering analyses of Kevlar have determined a series of well defined peaks, or

bands, ranging from 600 to 1700 cm^{-1} for different vibrational modes shown in Table 2-1 [12, 13]. Since Kevlar has a well defined Raman response, there have been many studies performed that characterize the structure of the polymer material and evaluate the material under applied strain [1, 12, 14-17].

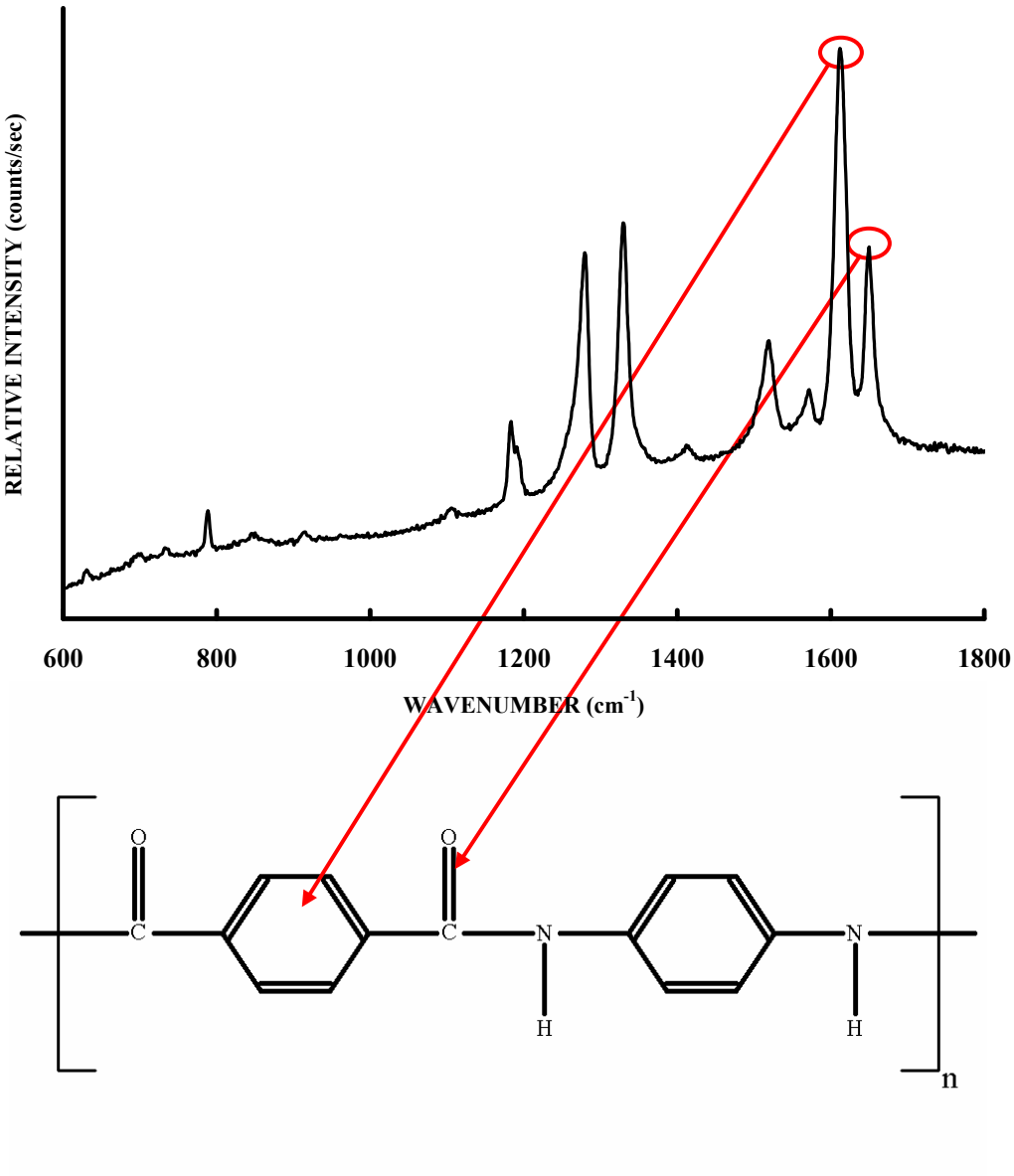

Figure 2-5. Raman spectrum of Kevlar. The vibrational modes of the 1613 and 1651 cm^{-1} bands are indicated.

The majority of previous studies on the material have analyzed the 1613 cm^{-1} peak due to the high sensitivity of the peak shift under applied strain, high intensity relative to other peaks in the spectrum, and relevance to the fundamental structure of the polymer, i.e. being produced by vibrations of the phenyl ring. The vibrational mode of the 1613 cm^{-1} band is from the C-C stretching mode of the phenyl ring. A phenyl ring is a member of the aromatic family of compounds.

Table 2-1. Raman bands of Kevlar and the corresponding vibrational modes [18].

WAVENUMBER (cm^{-1})	**BAND ASSIGNMENT**
630, 732, 786	Ring vibrations
845	C-H out-of-plane bending
863	Ring vibrations
1103	C-H in-plane bending
1181, 1277, 1327, 1514	C-C ring stretching
1318	C-H in-plane bending
1569	Amide II (60% N-H bending; 40% C-N stretching
1610	C-C ring stretching
1648	Amide I (80% C=O stretching; 10% C-N stretching 10% N-H bending)

The Raman spectrum of Kevlar 49 fibers under tensile stress was first reported by Penn and Milanovich [12]. Raman bands were first assigned to vibrational modes of the Kevlar polymer by using model monomeric compounds and known structure-absorption correlations. The fibers were then stressed in tension, and no significant changes in the Raman spectrum were reported. However, Galiotis et al. [16] observed that the whole Raman spectrum between 1100 and 1700 cm^{-1} (six Raman bands) shifted to lower frequencies with applied tensile strain for Kevlar 49 fibers. The rates of peak shifting were different for all six major peaks; with the 1613 cm^{-1} Raman band exhibiting the

highest sensitivity. The broadening of the Raman bands with applied tensile stress was also reported.

Prasad and Grubb [19] found a decrease in wavenumber and an increase in the Raman band width with sustained applied tensile strain for Kevlar 49 fibers. At a molecular level, when the fiber was stressed changes occurred in bond length and bond angle which may be observed on the Raman spectrum as shift in peak frequency. The band broadening may be created from defects in the fiber or defects being created in the fiber under stress. The load is transferred by secondary hydrogen bonds between the long chains of molecules. If there are defects present, the stress redistribution should create a greater increase in bandwidth. The number of defects in a Kevlar fiber is increased by exposure to ultraviolet (UV) light [19]. Raman bands have shown an increase in band broadening under applied load when fibers have been exposed to UV lighting.

Raman measurements were made comparing a stressed aramid fiber in air to a stressed aramid fiber post-cured in resin. These aramid fibers were Twaron type 1001 fibers which are similar to Kevlar 49. Ding and Varlow [20] discovered that the 1613 cm^{-1} Raman peak shifts at different rates for the fiber in air compared to the fiber in a resin matrix, concluding that the matrix significantly influences the material behavior. Aramid composite strands were also post-cured in resin; a single strand at room temperature and a strand at elevated temperature. The composite strand post-cured at elevated temperature was more sensitive to stress than the strand post-cured at room temperature, and it was concluded from this data residual stresses do exist.

The effect of water absorption on Kevlar 49 may be studied with Raman spectroscopy since the spectrum of water is weak and causes no interference [18].

Raman spectra were analyzed for Kevlar 49 fiber composite strands immersed in water at room temperature. Kawagoe et al. [17] applied tensile stress to a dried sample of Kevlar 49 fibers impregnated in an unsaturated polyester matrix, and to a Kevlar composite strand immersed in water. The rate of peak shifts appeared the same in both samples. However, through Fourier transform FT infra-red (FTIR) microscopy, where water is active, water molecules continued to exist under drying conditions. FTIR microscopy is an absorption measure, and is the inverse of Raman spectroscopy. If a material has a certain vibrational mode in FTIR, it does not have Raman scattering. Another study by Stuart [18] examined Kevlar immersed in water at room temperature using a FT Raman system. The intensity of each band was taken as a ratio by fixing the intensity of the 1278 cm^{-1} band to 1.00. A decrease in intensity of the 1613 cm^{-1} band was found for the sample immersed in water. The loss of intensity for this band was related to the disruption of hydrogen bonding resulting from immersion in water.

3

EXPERIMENTAL

3.1. Instrumentation

The Raman spectra reported here were measured using two separate instruments. A Renishaw micro-Raman system was used to measure Kevlar 49 fibers and fibers impregnated in an epoxy matrix with an incident laser of 488 nm, 647 nm and 752 nm (Figure 3-1a). The schematic diagram for the Renishaw Raman system was previously shown in Figure 2-4. The multi-frequency spectrometer enables the study of wavelength effects such as fluorescence. The laser source illuminates the sample surface through a 50x microscope objective. Raman scatter light is collected from the surface and a spectrometer with a CCD detector is used to evaluate the intensity of the Raman scattered light over a range of wavelengths. The collection time was generally averaged over two to three scans in the 600 to 1800 cm^{-1} region for 30 seconds each with a resolution of ~1.6 cm^{-1}. The Raman instrument was calibrated using a silicon sample due to its well-defined peak at 520 cm^{-1}.

Raman measurements were also taken using a Fourier Transform (FT) Raman system using an incident laser of 1064 nm (Figure 3-1b). The FT Raman system differs from the spectroscopic system in the determination of the wavelength of scattered light, which is determined by an interferometer rather than by a spectrometer. FT Raman systems use of the 1064 nm laser removes fluorescence completely. In the near-infrared (IR) region of 1064 nm, the photon energy is usually not sufficient to cause transitions between electronic states that give rise to fluorescence. For each spectrum, 32 scans were Fourier transformed with a resolution of 1.5 cm^{-1}. All spectra were analyzed using the commercial software Peakfit®.

(a)

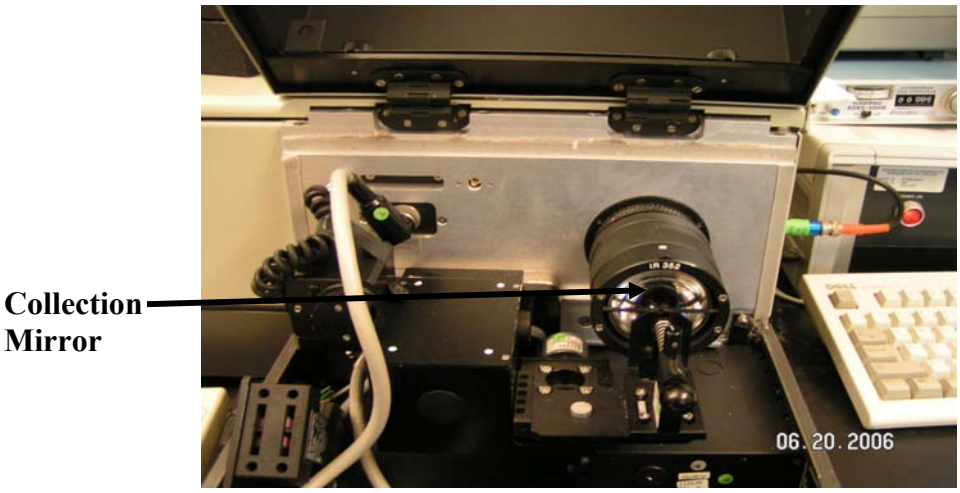

(b)

Figure 3-1. Two Raman systems were used for measurements (a) multi-laser Renishaw Raman spectrometer and (b) FT Raman system.

3.2. Materials and Testing

3.2.1. Aged Kevlar Samples

A series of Kevlar strand and composite samples have been evaluated to identify and characterize the Raman spectra. This has included virgin Kevlar yarn, virgin yarn impregnated in an epoxy matrix to form a Kevlar composite strand, and composite strand specimens that have been exposed to a creep testing regimen. Sections of composite

materials removed from aged fleet leader tanks and strand specimens aged by the Stepped Isothermal Method (SIM) have also been tested.

Five types of strand specimens have been provided by Texas Research International (TRI) as part of the study. This includes virgin Kevlar 49 yarn and composite strands that were initially used to explore the Raman response of the Kevlar materials and the effects of the matrix on the Raman response. TRI also provided a series of composite strand specimens that had been part of a creep testing program. During this program, a series of specimens were loaded to 65% of their tensile strength and held at load for various periods of time at different temperatures indicated in Table 3-1. Analysis focused on comparing a virgin composite strand labeled "D" from the table with strands that failed during creep testing.

Table 3-1. Details of Kevlar 49 creep tested specimen.

Creep Tested Composite Strands			
Specimen	**Aged (hrs)**	**Temp °C**	**Failed?**
A	9	92	yes
B	96	48	
C	48	48	
D	0	room	
E	96	20	
F	96	34	
G	50	76	
H	96	34	
I	1	90	yes
J	4	90	yes
K	9	92	yes
L	1	76	yes

SIM Kevlar composite strands were also provided by TRI and evaluated for changes in the Raman response. These SIM specimens were loaded to 65% of the ultimate tensile strength (UTS) in a temperature-controlled chamber. Step-wise increases in the temperature were imposed at sustained stress levels until failure [21]. The SIM Kevlar strands listed in Table 3-2 were tested at step-wise elevated temperatures initially at room temperature (20 °C). The strands were held under sustained load at 65% of the UTS for 10,000 seconds. If the strand did not fail, the temperature would be increased by 14 °C for 10,000 seconds. This process would continue until failure and the total time recorded.

Table 3-2. Details of Kevlar 49 SIM tested specimen.

SIM Tested Specimen		
Sample	Total Time (sec)	Temp at Failure(°C)
14o5	58770	90
21o5	50480	90
23d5	68130	103
23o5	60210	104

Kevlar materials being used for winding tanks in a stress rupture study have been provided. This material is a Kevlar prepreg composite strand in cured and uncured conditions, and is referred to as ATK Kevlar prepreg strands.

Finally, two samples of composite materials sectioned from burst COPVs were tested. These COPVs were part of a fleet leader program that maintained exemplar vessels under pressurized conditions over the lifetime of in-service vessels of similar designs. A section of Kevlar composite cut from serial number (SN) 032 fleet leader tank

consisted of material that was aged for ~17 years at 80 °C (pressurized to 50% ultimate tensile capacity, 29 MPa). This darkened material was removed from a tank that had burst during accelerated testing and was being analyzed at Cornell University. The spectra of a fleet leader sample that had been aged at room temperature (29 MPa) and then subject to a burst test was also evaluated. A sample from SN 007 fleet leader tank supplied was a layer cut out of a tank at ~0.1 inches in depth in the COPV. This specimen contains darkened fibers associated with manufacturing processes.

It is important to note that all samples tested were not under stress while scanned. Pictures of all specimen types are shown in Figure 3-2.

(a)

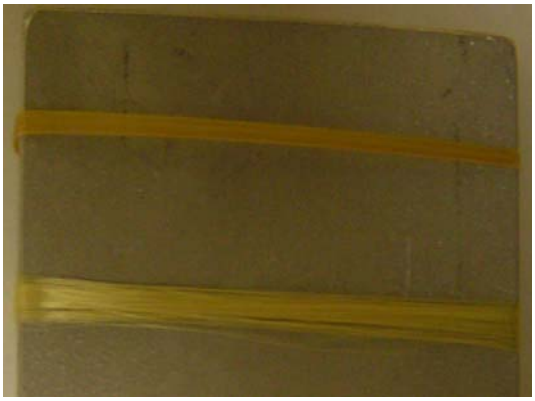

(b)

(c)

(d)

(e)

(f)

Figure 3-2. Kevlar 49 specimen (a) ATK strands (b) TRI strand and yarn (c) fleet leader SN 032 (d) fleet leader SN 007 (e) creep tested (f) SIM tested

3.2.2. Power and Polarization Testing

Problems arise when too much laser power is incident upon Kevlar samples. Literature indicates that the power of the incident laser may damage Kevlar fibers if above ~16 mW [12, 19]. Galiotis et al. [22] also studied the effects of incident power levels concluding that incident powers of 10 mW and greater can easily damage the fiber, possibly from local heating effects. As a result, the power levels have been closely controlled and kept at less than 10 mW on the sample surface when using the Renishaw Raman system. The lowest power that gives the best suitable spectrum was determined using a virgin strand of Kevlar 49. Power measurements were made at the sample surface using a handheld laser power meter to supplement instrumentation readings. This handheld device was used to ensure the power stayed well below 10 mW. It is important to note that the laser power is kept constant through a series of experimental analysis. Figure 3-3 shows spectra at different power levels. From the figure the most well-defined spectrum was at a power level of 7 mW.

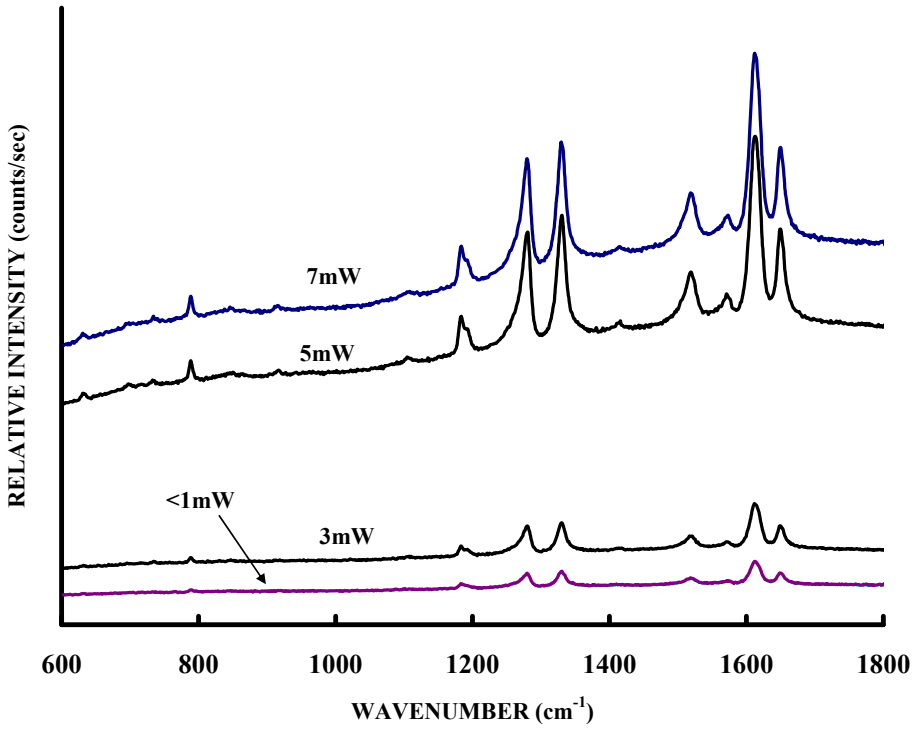

Figure 3-3. Raman measurements taken at different power levels.

Literature also indicates the molecules of Kevlar are highly oriented and as a result, the polarizability of the material is highly dependent on its orientation relative to the polarization of incident light. Testing was conducted to ensure the proper alignment of specimen in the micro-Raman system to ensure the most intense Raman spectra from the material. A Kevlar composite strand was mounted to a rotating device shown in Figure 3-4. The fiber was scanned with the Renishaw sytem from 0 to 360° in 10° intervals. Figure 3-5 displays two views of a Kevlar strand under the Raman microscope rotated at different angles. Figure 3-6 is a plot of the differences in appearance of the spectrum when the laser is polarized parallel to the fiber axis and perpendicular to the

fiber axis. Raman peaks are nearly indistinguishable from the background noise when the laser is polarized perpendicular to the fiber axis.

Figure 3-4. Rotating apparatus used for fiber alignment Raman measurements.

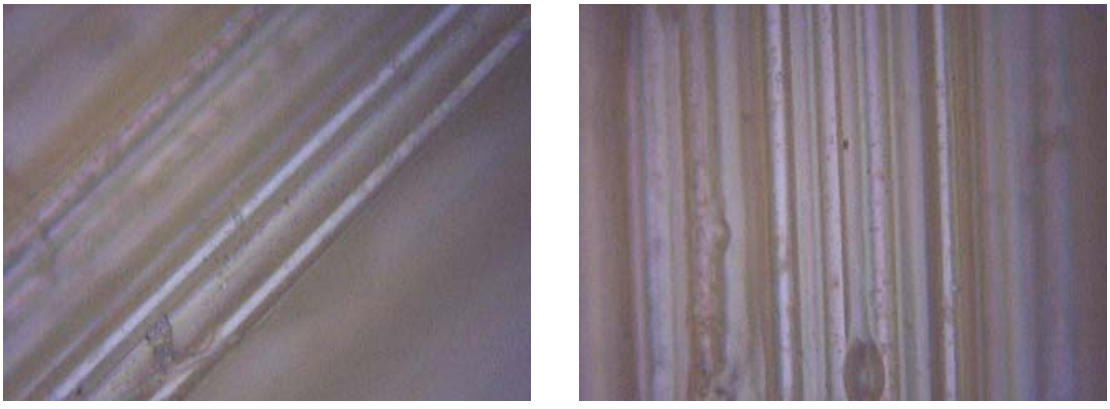

(a) **(b)**

Figure 3-5. A Kevlar 49 strand under a Raman microscope at (a) 45° and (b) 90°.

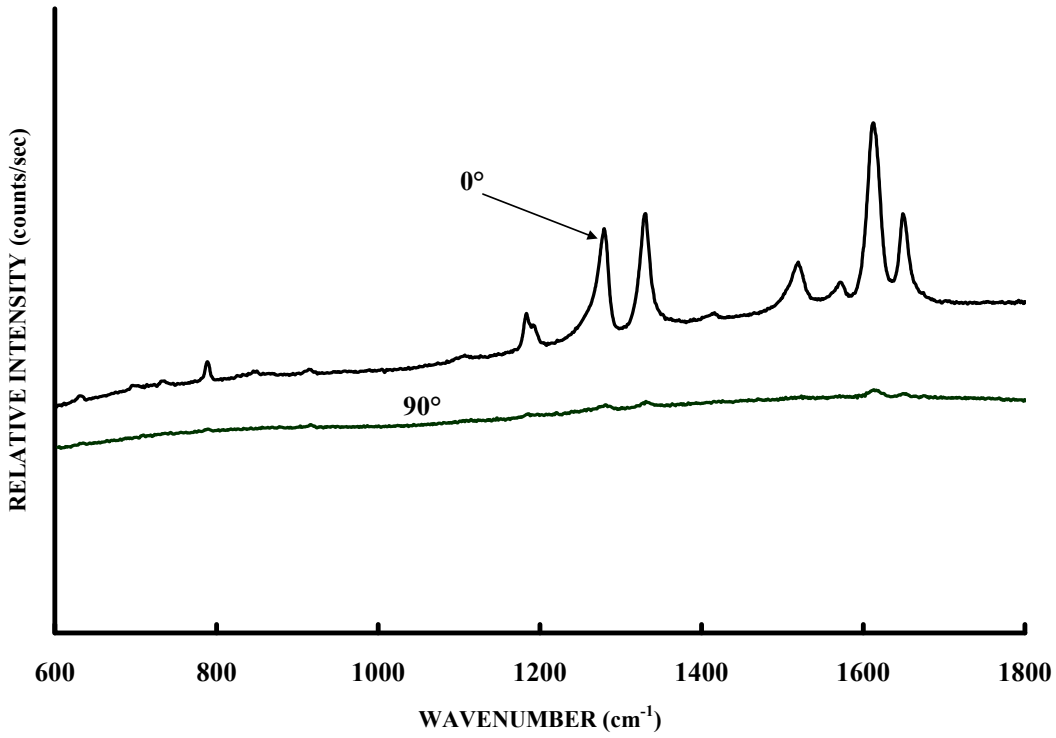

Figure 3-6. Raman spectrum of a Kevlar strand aligned at 0° and 90°.

It is important that all measurements using the Renishaw system attempt to focus the microscope directly on a fiber that is noticeably scattering the most light. When looking under the microscope at a Kevlar strand shown in Figure 3-5, if the laser is focused directly on a lighter area primarily at the fiber surface, the Raman spectrum will be well-defined. If the laser is focused on a darker area, the intensity of the Raman peaks will be low due to the laser directed primarily on the resin at the surface.

A particular challenge for Kevlar strands is that the fibers of Kevlar within the matrix provide strong, detailed spectra while the epoxy resin primary produces some fluorescence and irrelevant scattering. When tested through the objective of a

microscope, as was done here, the focus of the incident laser spot includes some combination of matrix and fibers, the fibers being at different varying depths in the matrix due to the texture of the strand surface. From Figure 3-5 the micrograph of the surface of a Kevlar strand is shown which illustrates the texture and the contrasting areas of matrix and fibers on the surface of the specimen. For different locations on a strand, there are different proportions of fibers at the surface and matrix at the surface. As a result, there is variation in the overall appearance of the spectra from scans at different locations on the same strand. The normalization techniques described later address this variation from scan to scan.

3.2.3. Mechanical Stress Testing

Individual virgin Kevlar strands were mounted to tabs using a quick-setting epoxy. The strands were then placed in a loading frame with a cylindrical load cell shown in Figure 3-7. Data was collected using the data acquisition commercial software Agile-link®. Raman spectra were obtained during deformation using a 647 nm krypton laser with the beam polarized parallel to the fiber axis for all measurements. Power was kept under 10 mW to prevent fiber damage.

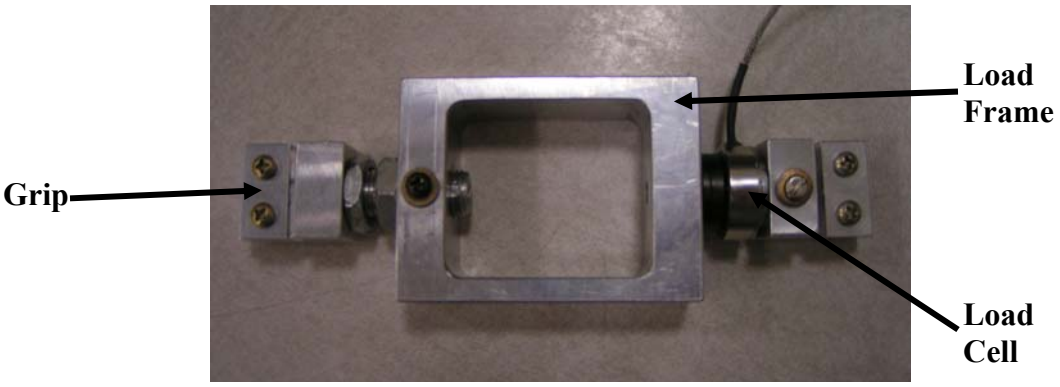

Figure 3-7. Loading frame and cylindrical load cell used for stress measurements.

3.2.4. Spectral Analysis

Quantitative characterization of Raman spectra requires the specific characteristics of spectra be identified, such that spectra from different samples can be normalized and compared. A common method of comparing spectra is to analyze the shifting of individual peaks to either a higher or lower wavenumber. Changes in the peak position may be indicative of changes in structure of the material or stresses within the material [1, 14-17, 19, 23, 24]. For the present study, peak positions were analyzed as well as the bandwidth and the relative intensity of the peaks. This section describes the primary characteristics of the spectra examined in this study and how these characteristics were analyzed to detect changes associated with the aging processes used.

The position of peaks within the Raman spectra was determined by Lorentzian curve fitting, using a best-fit curve with a Lorentzian fitting function. The process identifies the wavenumber of each peak in the spectrum that can be separated from the background noise, which is always present at some level. Algorithms are available in

commercial software. For Kevlar, there are between 8 and 16 individual peaks that can be identified in the range from 600 to 1800 cm^{-1}, depending on the wavelength of the incident laser. Some of these peaks are quite low in intensity and therefore more difficult to locate on the spectrum consistently. To evaluate the shifting of peaks, the peak positions (i.e. absolute wavenumbers) were normalized by comparing the position of individual peaks with the peak located at ~1613 cm^{-1} within a particular spectrum,

$$\Delta k_i = k_i - k_{1613}$$

Where:

k_i = Wavenumber of peak i, cm^{-1}

Δk_i = Shifting peak k_i relative to the 1613 peak, cm^{-1}

k_{1613} = Wavenumber of the ~1613 peak, cm^{-1}

The position of the ~1613 cm^{-1} peak can vary slightly from one spectrum to another, particularly when the instrument is recalibrated in between measurements. In this case, the entire spectrum may be shifted, such that the absolute position of a particular peak is inadequate for analysis. If the entire spectrum shifts from vibrational changes to the Kevlar, these shifts will be detected due to peaks shifting at different rates [14, 22]. The normalization of peak positions to the ~1613 cm^{-1} peak within the spectrum allowed for the quantitative comparison of position.

A second characteristic of the spectra analyzed was the full width, half maximum (FWHM) of individual peaks within the spectrum. For this measurement, the width of the fitting function is determined at ½ of the maximum intensity of the peak. This value is

then normalized by determining the ratio of the individual peak's FWHM to the FWHM of the ~1278 cm^{-1} peak for that spectrum:

$$\eta_i = \frac{FWHM_i}{FWHM_{1278}}$$

Where:

η_i = FWHM ratio (dimensionless)

$FHWM_i$ = FWHM of peak *i*, cm^{-1}

$FHWM_{1278}$ = FWHM of ~1278 cm^{-1} peak, cm^{-1}

Finally, the relative intensity of the individual peaks was analyzed. Each intensity value was determined then normalized by calculating the ratio of the individual peak's intensity to the intensity of the 1278 cm^{-1} peak for that spectrum:

$$\chi_i = \frac{I_i}{I_{1278}}$$

Where:

χ_i = Intensity ratio (dimensionless)

I_i = Intensity of peak *i*, cm^{-1}

I_{1278} = Intensity for ~1278 cm^{-1} peak, cm^{-1}

Characterization of the Raman spectrum was conducted using incident laser wavelengths of 488, 647, 752 and 1064 nm. In general, the shorter wavelength incident laser produces greater florescence, and consequently lower signal to noise ratio, than longer wavelengths. For analysis, the 647 and 1064 nm incident lasers were selected

because these incident wavelengths provided both fine spectra and a broad range of wavelengths for analysis.

The analysis of relative peak intensity and FWHM was conducted by comparing the average values from a series of between two and five separate scans of a strand specimen, from multiple locations on the surface of the strand. This average provided a typical value for the strand. This process also allowed for some measure of the variation of results that could occur when evaluating multiple measurements of the same strand.

4

RESULTS

4.1. Comparison of Spectra

Figure 4-1 indicates the Raman spectra at 647, 752 and 1064 nm, and Figure 4-2 indicates the Raman response at 488 nm for virgin (unaged) Kevlar strands. The latter figure illustrates the increased background noise associated with fluorescence and specimen heating at shorter wavelengths such as the 488 nm laser. As shown in the figures, clear Raman spectra can be obtained at each incident wavelength, though there is significant background noise at 488 nm.

Major problems arise in obtaining a Raman spectrum due to fluorescence for most polymers when using a 488 nm argon laser. Fluorescence is a luminescence in which the molecular absorption of a photon triggers the emission of another photon with a longer wavelength. This results in a change in energy between the absorbed photon and emitted photon, transformed to molecular vibrations or heat. It is possible to avoid fluorescence problems by changing the incident laser frequency to a krypton laser at 647.1 nm or a near-IR Nd:YAG laser at 1064 nm. The former sets the excitation frequency below the

fluorescent envelope and the latter is a more drastic approach using the FT Raman technique which is in the IR region that is far below the absorbing electronic frequencies [10].

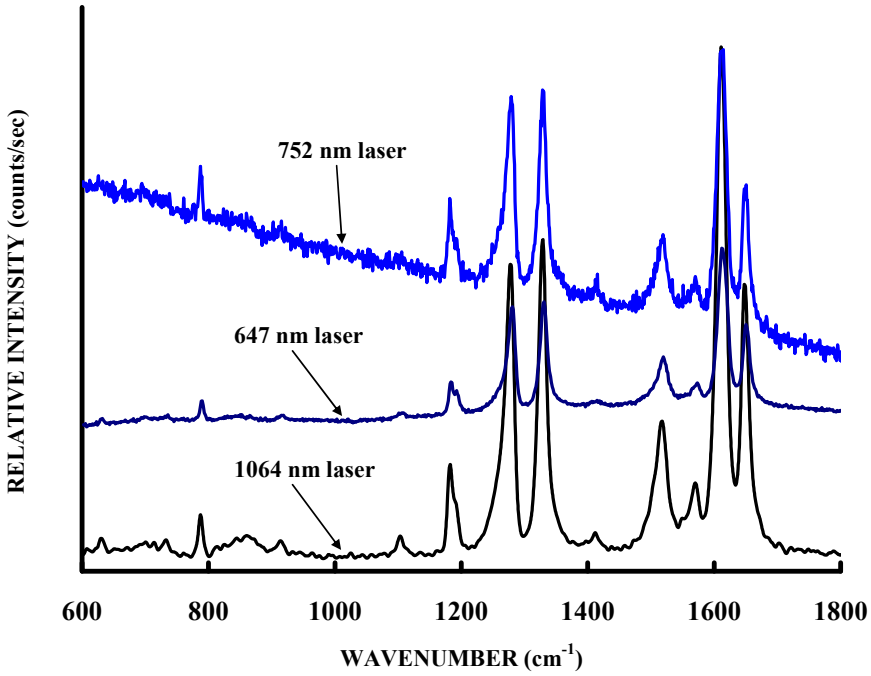

Figure 4-1. Raman spectrum of a Kevlar 49 strand using an incident laser of 647, 752 and 1064 nm.

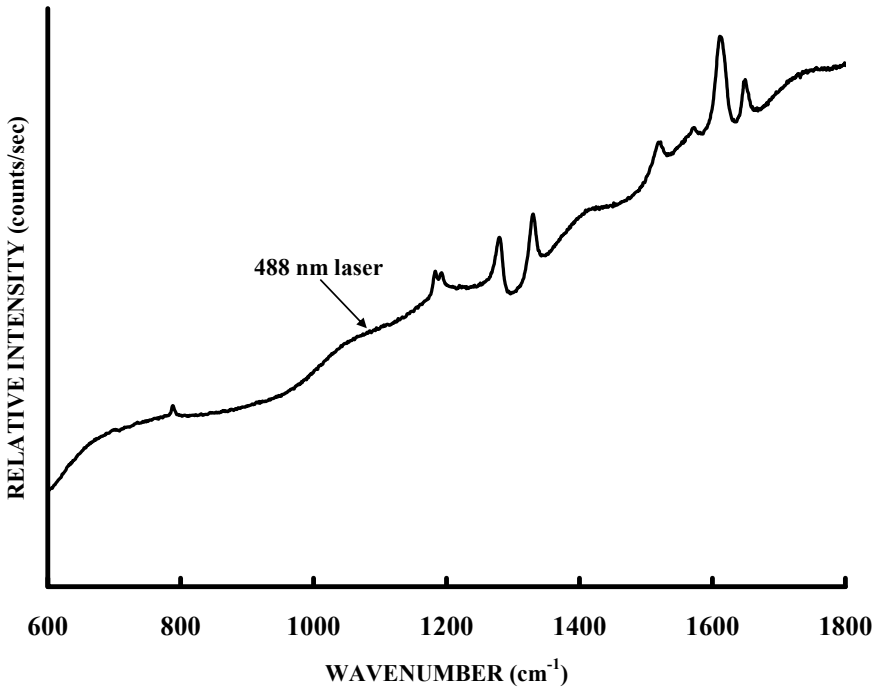

Figure 4-2. Raman spectrum of a Kevlar 49 strand using a 488 nm incident laser.

4.2. Raman Band Detection

Analyses were conducted of the obtained spectra compared with spectra described in the literature[12, 13]. Matching experimental Raman band or peak values with those provided in the literature, it was found that in the range of 600 to 1700 cm^{-1} there was significant agreement. Table 4-1 lists the theoretical peaks compared to the experimental peaks. Experimental peak values could be related to 13 out of 14 of Penn and Milanovich analytical peaks, and 14 out of 15 for Kim et al. analytical peaks using an incident laser wavelength of 752 nm. Using the FT Raman system with an incident laser

wavelength of 1064 nm, all theoretically predicted peaks could be identified. There was slightly less agreement using an incident wavelength of 647 nm, finding 13 out 14 peaks predicted by Penn and Milanovich and 13 out 15 of the peaks predicted by Kim et al. There was significantly less agreement with an incident laser of 488 nm. For shorter wavelengths, small peaks are more difficult to identify and may be lost in the background noise evident in Figure 4-2, and as a result these peaks are not identified.

Table 4-1. Comparison of theoretical and experimental Raman peaks of Kevlar 49.

RAMAN PEAKS (cm^{-1})						
TEST TYPE						
Theoretical		**Kevlar yarn**	**Kevlar strand**			
Penn and Milanovich Peaks	**Kim et al. Peaks**	**(647 nm)**	**(488 nm)**	**(647 nm)**	**(752 nm)**	**(1064 nm)**
632	**637**			631	630	630
698	**694**			700	697	695
734	**725**			731	732	732
789	**773**	790	784	789	787	787
-	**853**				847	845
-	**-**	914		915	913	918
1104	**1106**	1105		1105	1105	1108
1187	**1187**	1184	1186	1184	1185	1186
1192	**1188**					1194
1279	**1283**	1280	1278	1280	1278	1283
1331	**1332**	1331	1331	1330	1329	1332
1409	**1400**	1413		1411	1415	1417
1518	**1516**	1519	1520	1518	1517	1521
1570	**1567**	1572	1577	1571	1570	1574
1615	**1615**	1613	1612	1613	1612	1615
1649	**1654**	1649	1649	1649	1649	1651

It is interesting to note a peak was found at ~915 cm^{-1} using the 647, 752 and 1064 nm lasers, but was absent in the literature. This peak was found in the Kevlar yarn

as well as strand, eliminating the possibility that this is a resin effect. This peak was not identified in using an incident wavelength of 488 nm. This ~915 cm^{-1} peak was relatively low in intensity, and is likely not apparent due to the low S/N ratio using the short wavelength laser. This peak may result from remaining moisture in the composites when processed, or absorbed following processing.

4.3. Spectra Characteristics

Analysis of the Raman spectra was conducted. The characteristics of the Raman spectra that were investigated included shifts in Raman peak values (Δk_i), changes in full width at half maximum (FWHM) of Raman bands (η_i), and normalized peak intensity variations (χ_i). Shifts in peak values were determined using a best-fit curve with a Lorentzian fitting function. The FWHM and normalized intensity values were determined by a similar approach but instead of a best-fit curve, a discrete value from the raw data was selected for the peak value based on the curve fit. The 647 and 1064 nm incident lasers were used for analysis because these incident wavelengths provided both fine spectra and a broad range of wavelengths for analysis.

4.4. Peak Shifting

The entire spectrum between 1100 and 1700 cm^{-1} shifted to lower wavenumbers under applied tensile stress for a virgin Kevlar composite strand. The 1613 cm^{-1} band showed the highest sensitivity with applied strain which is in direct agreement with the literature [14, 22]. The 1613 cm^{-1} band decreased ~1.5 cm^{-1} per 10 lbs of force. Figure

4-3 shows the decrease in wavenumber of the 1613 cm^{-1} band with applied tensile stress. A Raman spectrum illustrates the peak shifting shown in Figure 4-4. A line of best-fit has been inserted into the figure.

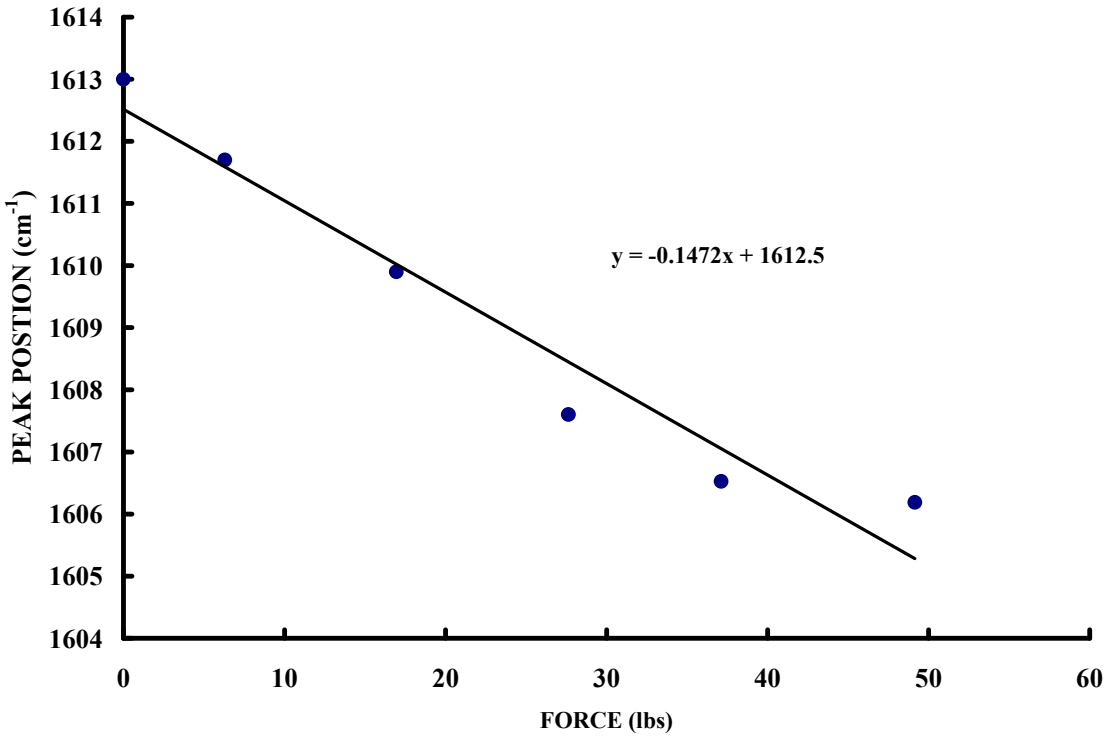

Figure 4-3. Force dependence of the 1613 cm^{-1} Raman peak for a Kevlar 49 strand. The straight line of best-fit was inserted into the data.

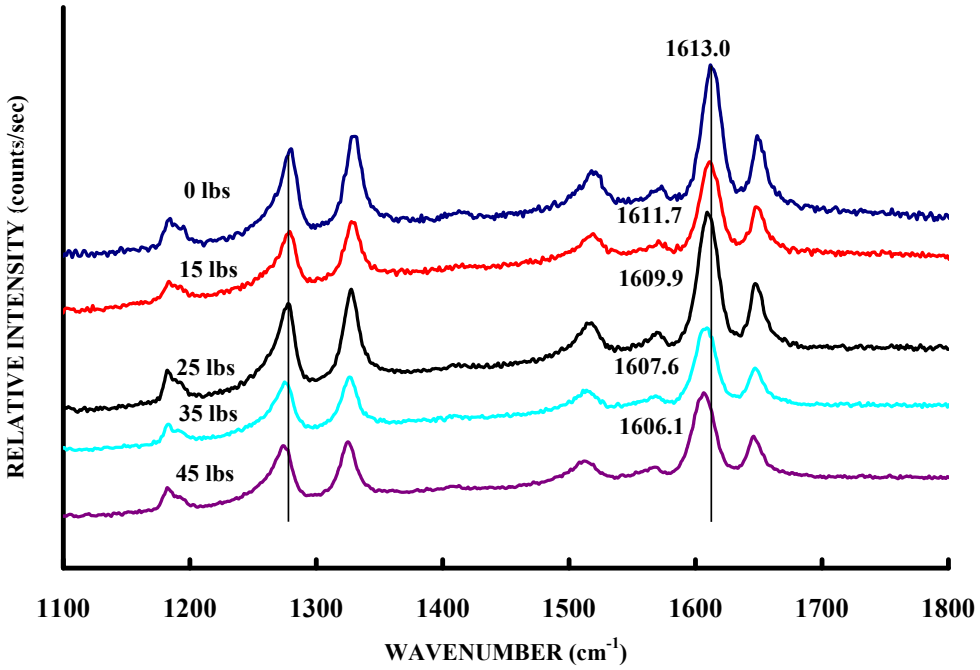

Figure 4-4. Raman spectrum of a Kevlar 49 composite strand at different loading levels. The 1613 cm^{-1} band shifts to a lower wavenumber.

To evaluate peak shifting for the aged specimens, each major peak value of a sample, k_i, was subtracted from the 1613 cm^{-1} peak, k_{1613}, of its own spectrum. Using this method, any shift in peak values would be detected due to the different rates that each peak shifts. No significant peak shifting was detected relative to the 1613 cm^{-1} peak. All 1613 cm^{-1} peak values were with a range of ± 0.05 cm^{-1} of the average value for a given data set. This variation was due to noise in the spectra and slight variations of calibrating the instrument, and could not be correlated with damage. The Raman system used is a multi-laser system that frequently has the incident laser changed, requiring

system recalibration. When the system is recalibrated, variation in results may occur. Results of this analysis using a 647 nm and 1064 nm laser are plotted in Figure 4-5 for virgin, creep, fleet leader, and SIM tested strands. The linear relationship and overlapping data shown in the figure indicates that individual peaks have not shifted relative to each other. It has been found that there are variations in the locations of peaks when using different wavelengths of incident light, but this is believed to be a measurement artifact.

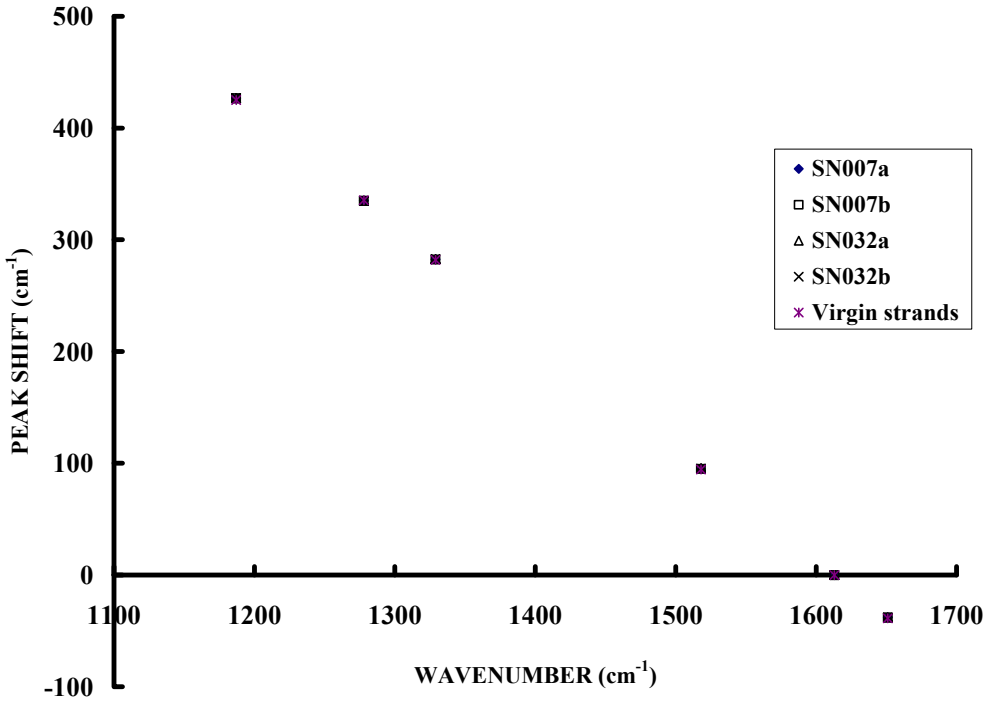

(a)

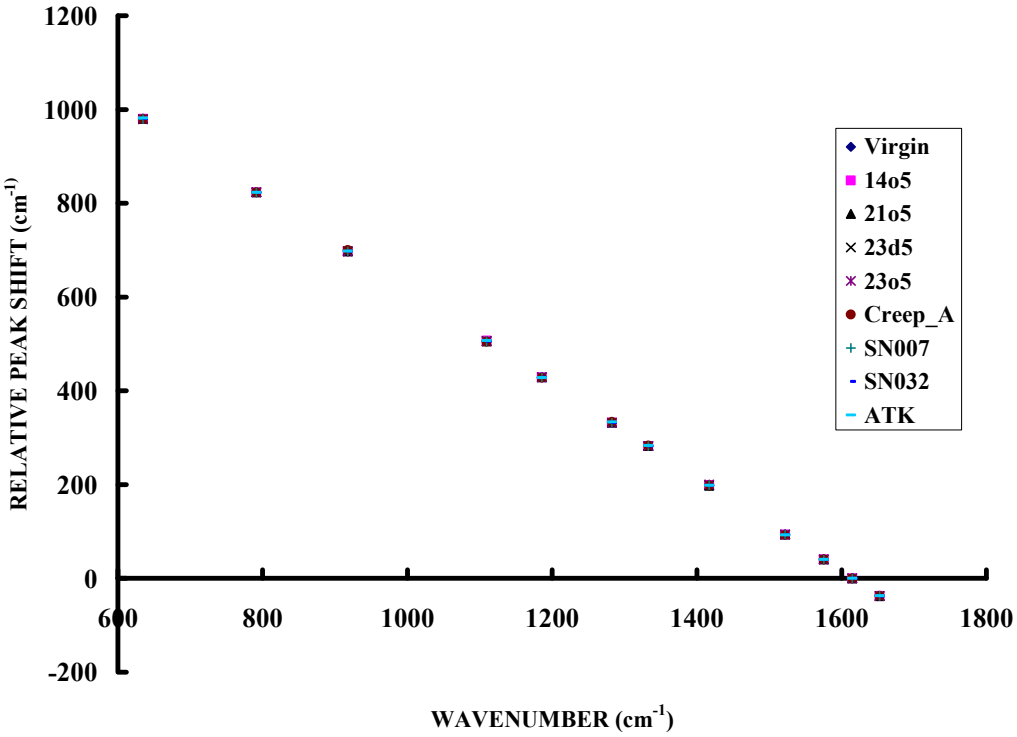

(b)

Figure 4-5. Raman peak positions were subtracted from the 1613 cm-1 peak position for virgin and aged Kevlar 49 strands using an (a) 647 nm laser and (b) 1064 nm laser.

4.5. FWHM

The full width at half maxima (FWHM) was analyzed for each major Raman band for the virgin, creep tested, SIM, and the fleet leader samples. For the incident laser of 647 nm, six Raman bands were analyzed: 1187, 1278, 1329, 1518, 1613, and 1651 cm^{-1}. Using the FT system, 12 Raman bands were analyzed including: 635, 791, 918, 1109,

1187, 1278, 1329, 1417, 1518, 1575, 1613, 1651 cm^{-1}. Figure 4-6 shows the FWHM ratio, η_i , on the vertical axis for each of the individual bands analyzed using the 647 nm incident laser. Virgin Kevlar strands and yarn produced spectra with low variations of FWHM ratios when comparing the two most predominant Raman peaks of 1331 and 1613 cm^{-1} (shown in Figure 4-6). From the figure, each data point represents an average of several measurements.

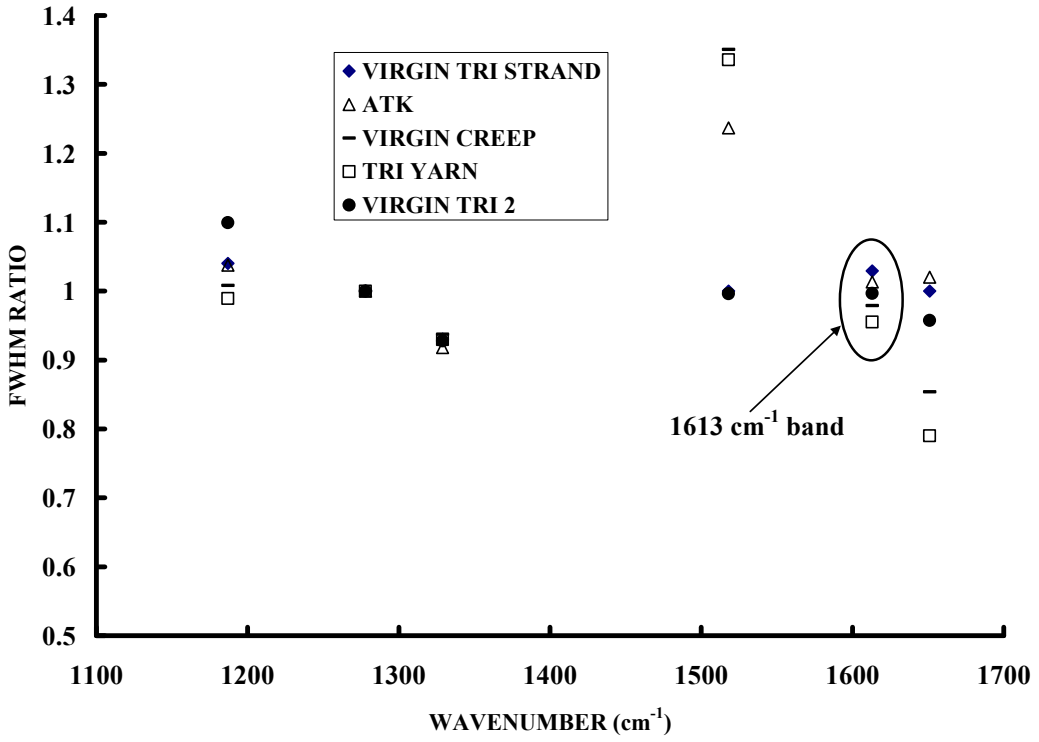

Figure 4-6. Variations of FWHM ratios for all virgin Kevlar specimens.

Figure 4-7a shows the FWHM results for the strand specimens that had been exposed to creep testing. The figure illustrates the results for each of the Raman bands that were analyzed, but particular attention is given to the ~1613 cm^{-1} band that is related

to the ring vibrations of the C-C phenyl ring and provides the backbone of the Kevlar microstructure. As shown in Figure 4-7a, the FWHM ratio for the creep specimens appears to generally increase for most of the bands in the spectrum relative to the virgin, unaged specimen tested. The ~1613 cm^{-1} band increased up to 0.06, though one creep specimen illustrated a slight decrease in FWHM ratio. Although the FWHM was generally increased, one exception is the band at 1518 cm^{-1} that has a very broad peak as indicated by its high FWHM ratio. This particular band has a very low intensity, as shown in Figure 4-1. The low signal to noise ratio of this band results in a high variation in the bandwidth.

Figure 4-7b shows the FWHM ratio for the fleet leader specimens. These specimens are sectioned from COPVs that had been aged for a number of years, and likely provide the most realistic representation of aged materials. The FWHM has increased significantly for the 1613 cm^{-1} band, and in fact is increased for most of the bands analyzed when compared with the virgin specimen. The exception again is the 1518 cm^{-1}, a low-intensity band that shows high variation in results. The FWHM ratios of the 1613 cm^{-1} band are increased for the fleet leader samples up to 0.10.

In contrast to the creep and fleet leader samples, the FWHM of the SIM samples appeared to slightly decrease as shown in Figure 4-7c. This decrease may be due in part difficulties in measuring failed samples that have a low thickness relative to virgin samples used for comparison. These samples were also fractured during SIM testing, resulting in a frayed appearance. Proper orientation within the test apparatus was difficult to achieve. It is important to note that all virgin data points are from a precise calibration set. For example, in Figure 4-7 the virgin data points are from the same

calibration set as the creep tested specimen. Calibration of the instrument may change from other experimenters interchanging the incident lasers and therefore changing the optics causing slight variations in the data.

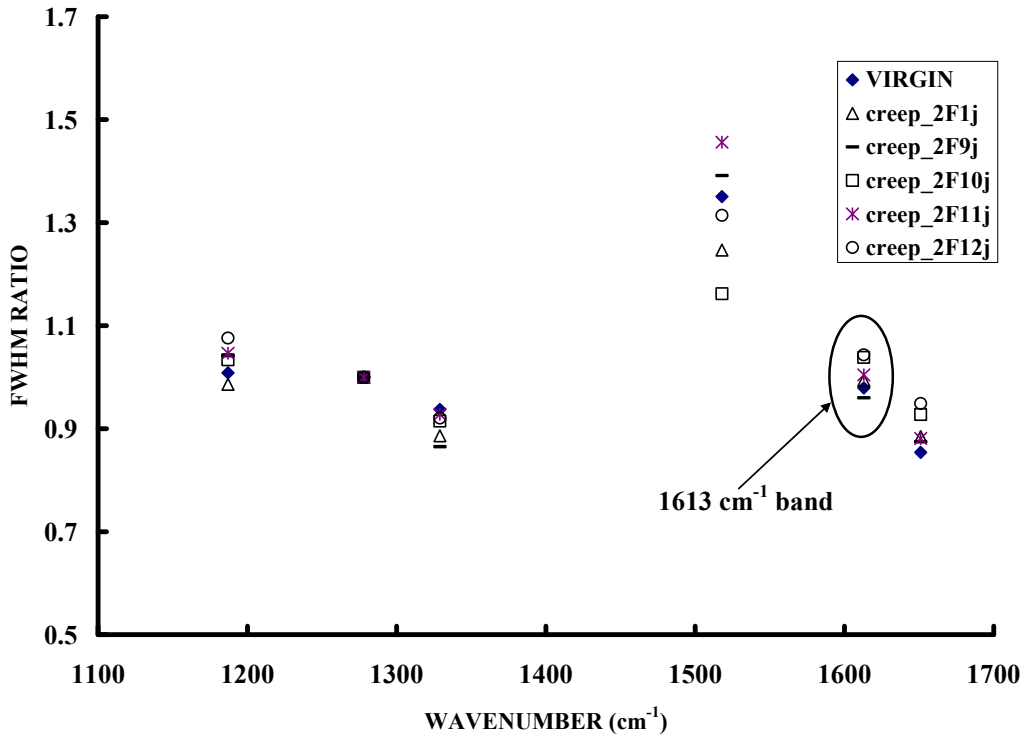

(a)

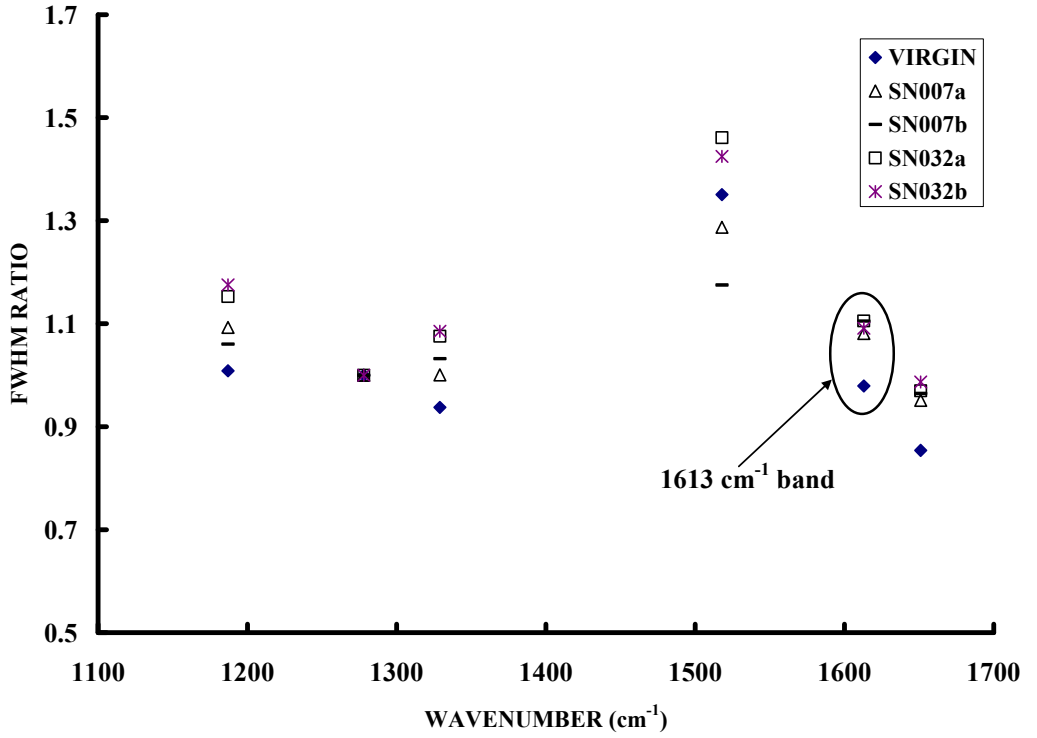

(b)

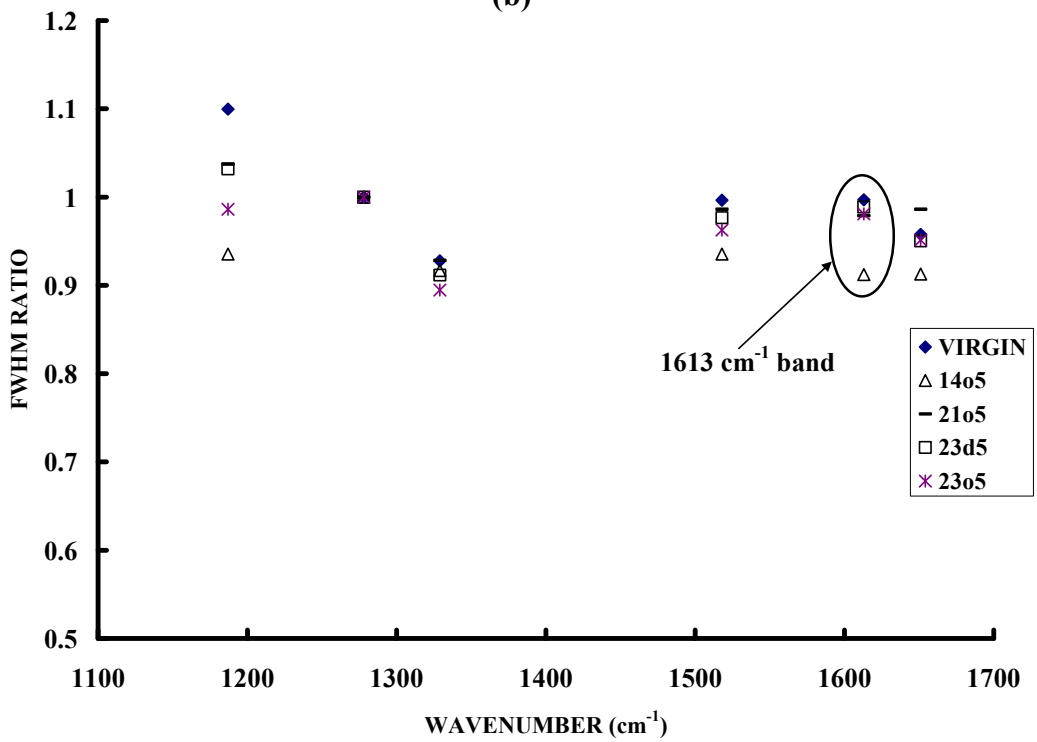

(c)

Figure 4-7. FWHM ratios of virgin Kevlar 49 strands compared to (a) creep tested specimens (b) fleet leader specimens and (c) SIM specimens.

No significant change in FWHM was found in the spectra obtained from the 1064 nm laser except for the very small peaks such as 1518 cm^{-1} band. These insignificant changes were found for FWHM when using the 1064 nm laser due to the narrow shape of the intense Raman bands; therefore the FWHM values are less sensitive to changes. Changes in the 1518 cm^{-1} band can be attributed to measurement error due to the difficulty in measuring this small peak.

4.6. Intensity

Intensity analysis was performed for virgin, creep, SIM and the fleet leader samples using a 647 nm laser and a FT setup with a 1064 nm laser. Figure 4-7 shows the relative intensity of each band compared with the relative intensity of bands from virgin specimens. Figure 4-8 shows the comparison of the relative intensities, χ_i, using the incident laser of the 647 nm for the creep, fleet leader and SIM specimens. Virgin Kevlar strands and yarn produced spectra with low variations of intensity ratios when comparing the two most predominant Raman peaks of 1331 and 1613 cm^{-1} (shown in Figure 4-7). From the figure, each data point represents an average of several measurements.

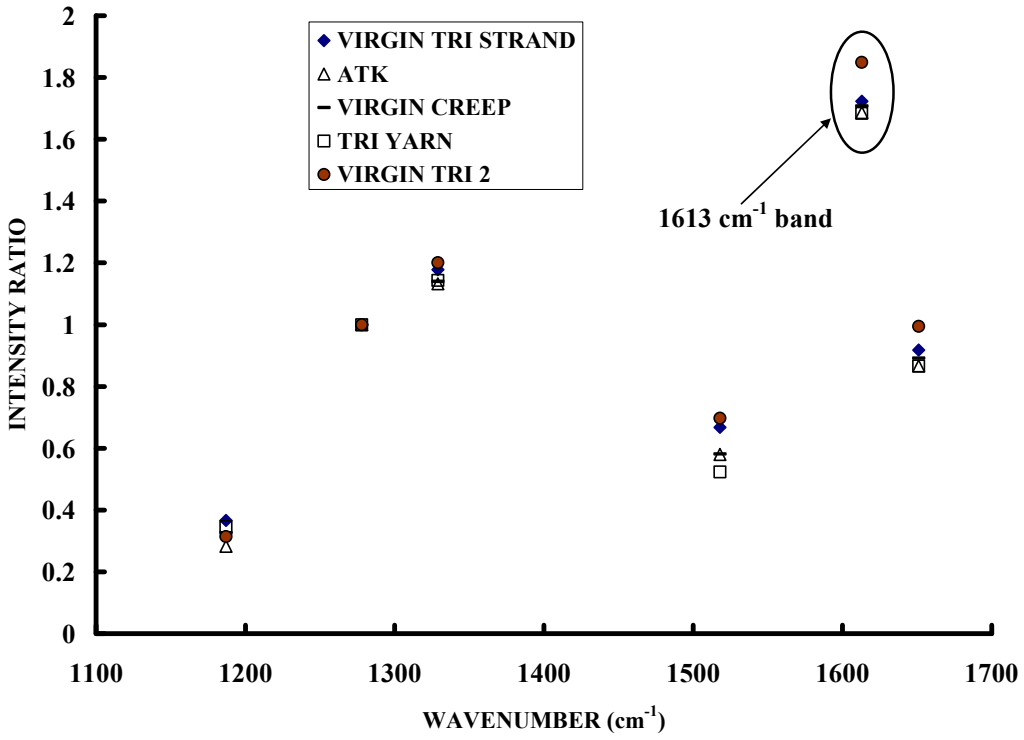

Figure 4-8. Variations of intensity ratios for all virgin Kevlar specimens.

Figure 4-9a provides results for the creep tested specimens. The results shown in this figure indicate that there was a reduction in the relative intensity of the 1613 cm^{-1} band for three of the four specimens evaluated. For the balance of the bands analyzed, there were mixed results when compared with the virgin specimens. For the fleet leader specimens, the results shown in Figure 4-9b indicate the intensity of the 1613 cm^{-1} band has clearly decreased for these specimens relative to the virgin strands. The effect appears more pronounced for specimens SN032a and SN032b, which were sectioned from a tank that had been aged at elevated temperature (80°C), up to $\chi_{1613} \approx 0.16$ for one of the specimens.

The results of testing SIM strands are shown in Figure 4-9c. As indicated in this figure, there is a significant reduction in the intensity ratio, χ_i, relative to the virgin SIM specimen for the 1613 cm^{-1} peak. For both fleet leader specimens and the SIM tested specimens, there was a similar decrease in the χ_i values for bands located at 1649 and 1330 cm^{-1}. The results using the FT Raman testing were consistent with the results of the 647 nm incident laser, namely that the intensity ratio was reduced for these specimens (Figure 4-10). The absolute minimum virgin value with the SIM specimens is plotted in Figure 4-11. This minimum value is the absolute lowest single measurement recorded of all virgin strand data for the intensity of the 1613 cm^{-1} peak.

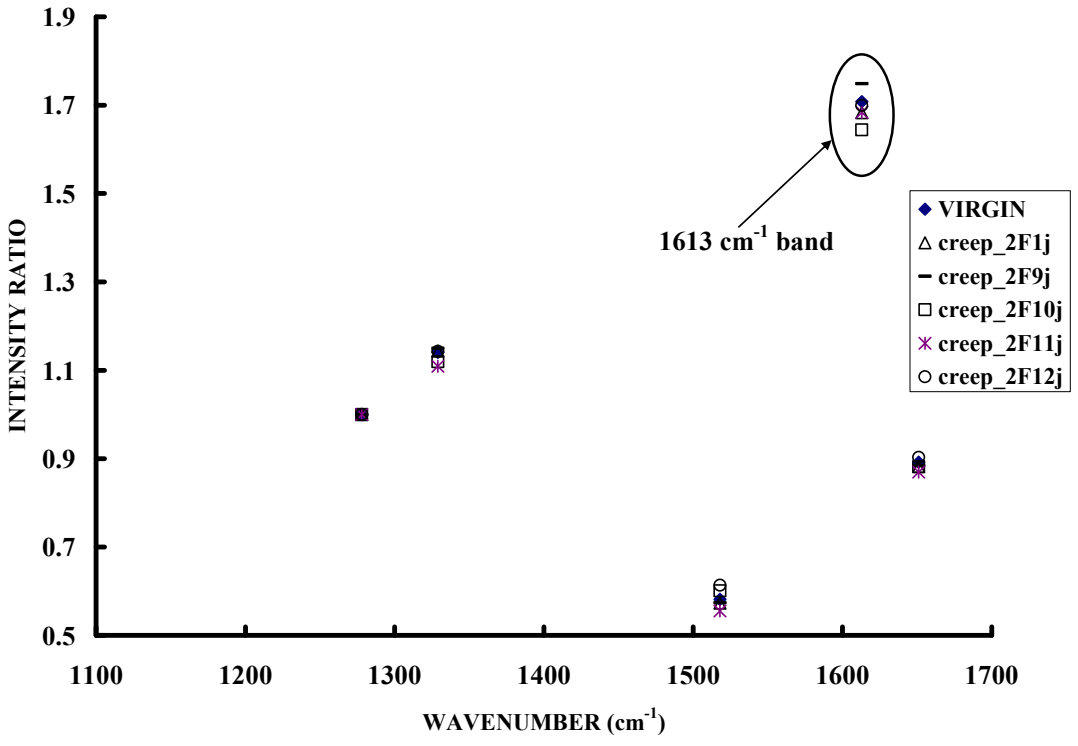

(a)

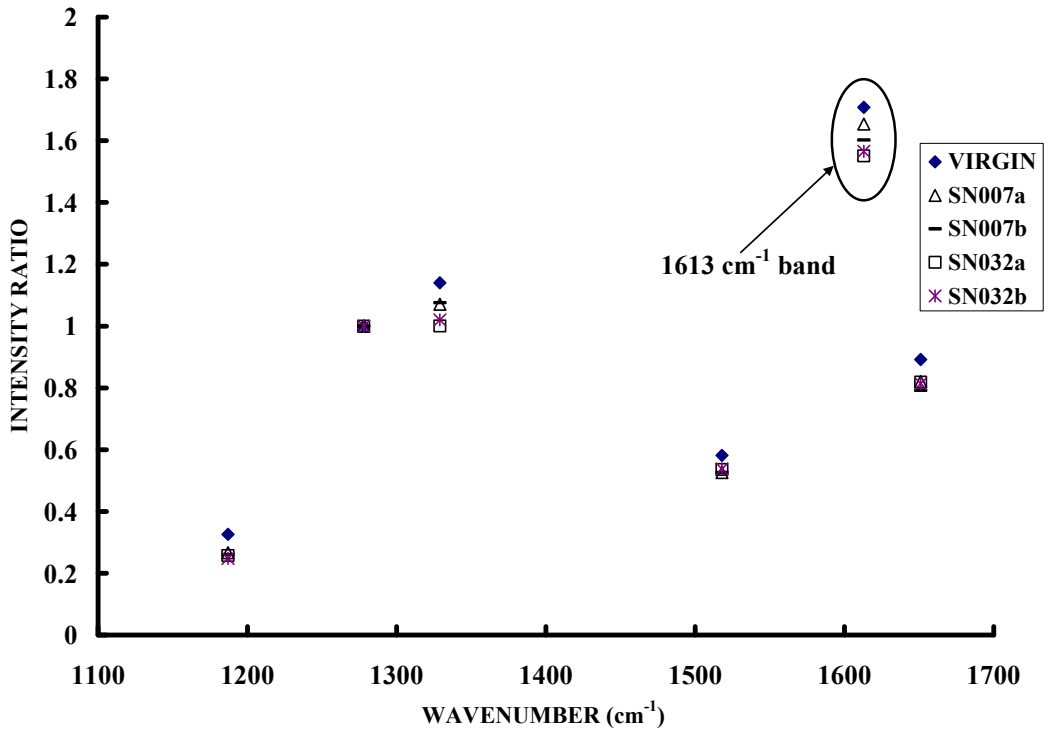

(b)

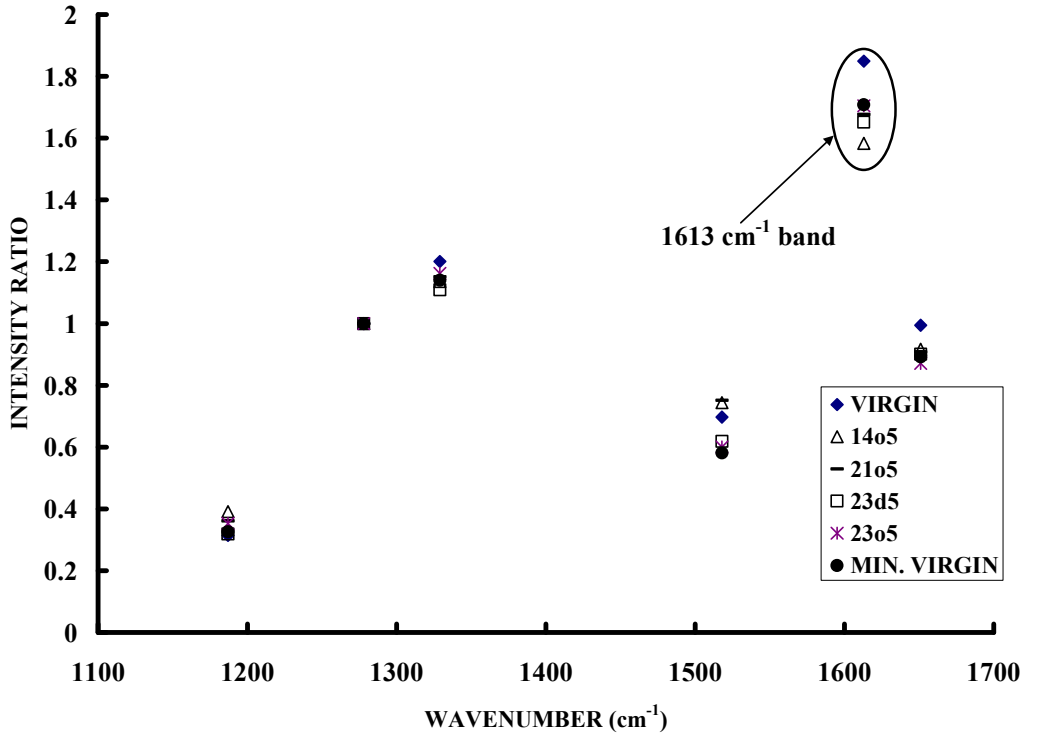

(c)

Figure 4-9. Intensity ratios of virgin Kevlar 49 strands compared to (a) creep tested specimens (b) fleet leader specimens and (c) SIM specimens. An incident laser of 647 nm was used.

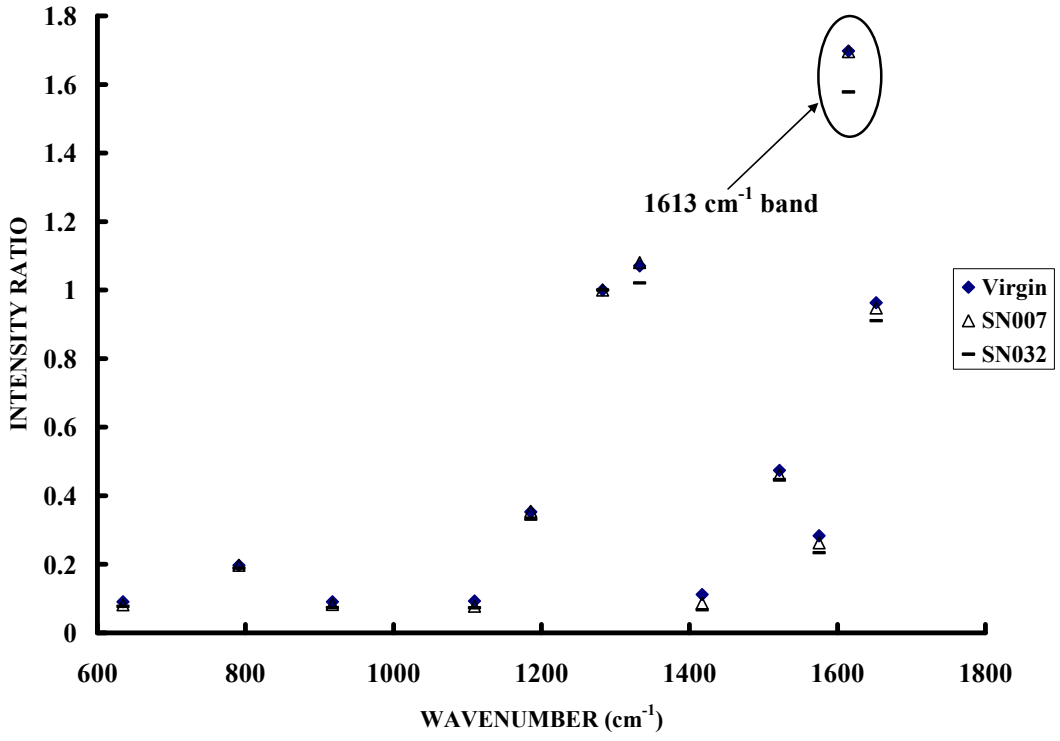

(a)

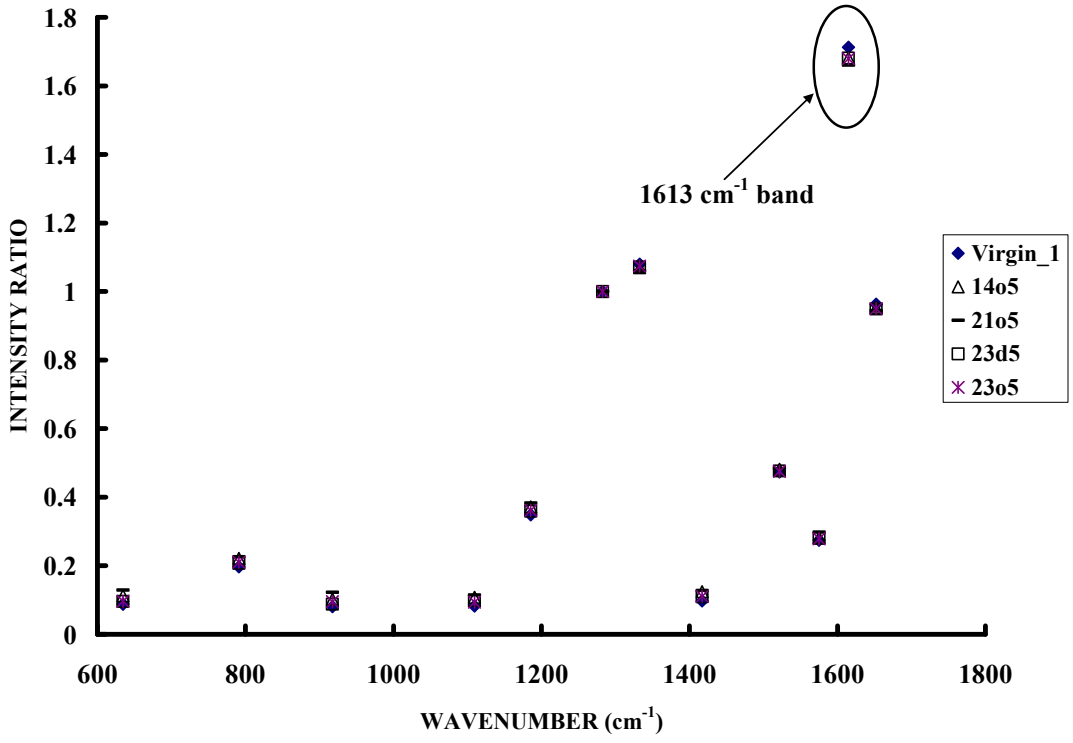

(b)

Figure 4-10. Intensity ratios of virgin Kevlar 49 strands compared to (a) fleet leader specimens and (b) SIM specimens. An incident laser of 1064 nm was used.

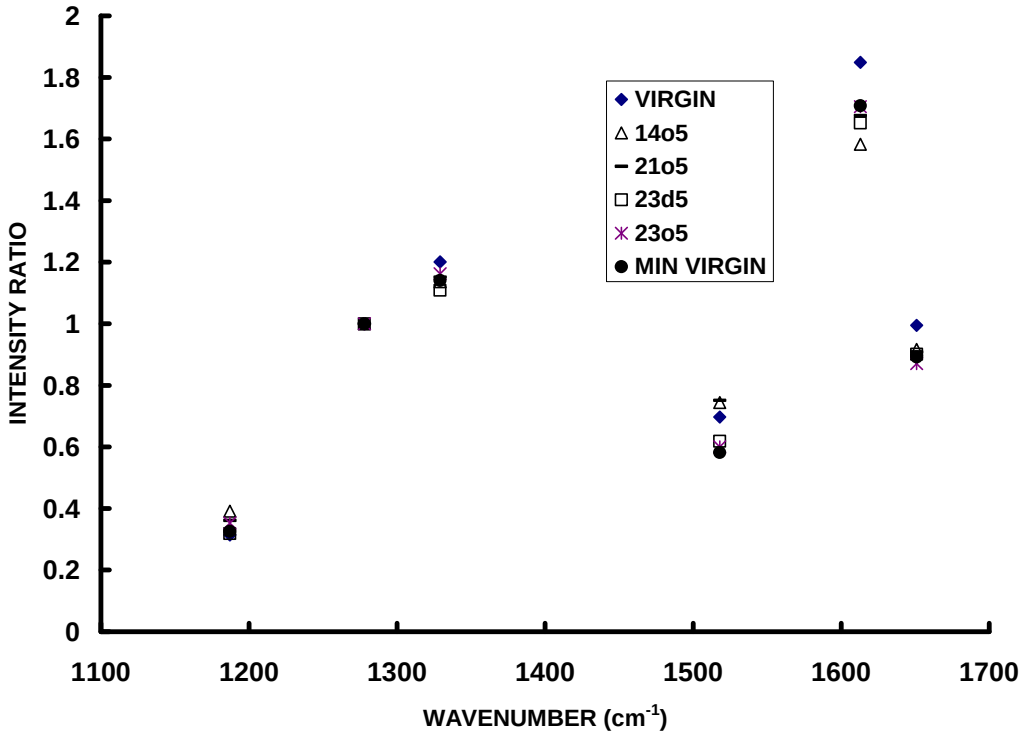

Figure 4-11. Intensity ratios of a virgin Kevlar 49 strand compared to SIM tested specimens using an incident laser of 647 nm. The minimum value for all virgin specimen measurements is labeled.

4.7. Data Summary

Creep, fleet leader and SIM samples were evaluated to detect any differences in the Raman spectra compared to virgin samples. The Kevlar virgin samples include TRI virgin strands, TRI virgin yarn, virgin creep strands, and ATK prepreg strands. All average normalized FWHM and peak intensity values for each sample type are tabulated in Tables 4-2 and 4-3**.** Table 4-2 represents results for a 647 nm incident laser and Table 4-3 represents results for a 1064 nm incident laser.

Table 4-2. Average values of intensity and FWHM ratios for all specimen types using a 647 nm incident laser.

	647 nm Laser											
	Intensity Ratio						FWHM					
Specimen	**1187**	**1278**	**1329**	**1518**	**1613**	**1651**	**1187**	**1278**	**1329**	**1518**	**1613**	**1651**
Virgin TRI Strand	0.34	1.00	1.19	0.68	1.79	0.96	1.07	1.00	0.93	1.00	1.01	0.98
Virgin TRI Yarn	0.35	1.00	1.14	0.52	1.68	0.87	0.99	1.00	0.93	1.34	0.96	0.79
Virgin Creep	0.33	1.00	1.14	0.58	1.71	0.89	1.01	1.00	0.94	1.35	0.98	0.85
ATK	0.28	1.00	1.13	0.58	1.69	0.87	1.04	1.00	0.92	1.24	1.01	1.02
Creep_A	0.32	1.00	1.14	0.57	1.68	0.88	0.99	1.00	0.89	1.25	0.99	0.88
SIM 14o5	0.39	1.00	1.14	0.74	1.58	0.92	0.94	1.00	0.92	0.94	0.91	0.91
SIM 21o5	0.36	1.00	1.15	0.75	1.68	0.91	1.04	1.00	0.93	0.99	0.98	0.99
SIM 23d5	0.32	1.00	1.11	0.62	1.65	0.90	1.03	1.00	0.91	0.98	0.99	0.95
SIM 23o5	0.35	1.00	1.16	0.60	1.70	0.87	0.99	1.00	0.89	0.96	0.98	0.95
SN007a	0.27	1.00	1.07	0.53	1.65	0.82	1.09	1.00	1.00	1.29	1.08	0.95
SN007b	0.26	1.00	1.08	0.53	1.60	0.79	1.06	1.00	1.03	1.17	1.10	0.96
SN032a	0.26	1.00	1.00	0.54	1.55	0.82	1.15	1.00	1.08	1.46	1.11	0.97
SN032b	0.25	1.00	1.02	0.54	1.57	0.81	1.18	1.00	1.09	1.42	1.09	0.99

Table 4-3. Average values of intensity and FWHM ratios for all specimen types using a 1064 nm incident laser.

	1064 nm Laser											
	Intensity Ratio						FWHM					
Specimen	**1187**	**1278**	**1329**	**1518**	**1613**	**1651**	**1187**	**1278**	**1329**	**1518**	**1613**	**1651**
Virgin TRI Strand	0.35	1.00	1.07	0.48	1.71	0.96	0.86	1.00	0.90	1.45	1.08	0.87
Virgin TRI Yarn	0.35	1.00	1.07	0.47	1.69	0.99	0.87	1.00	0.91	1.52	1.09	0.80
Virgin Creep	0.32	1.00	1.06	0.47	1.72	0.95	0.85	1.00	0.85	1.35	0.99	0.89
ATK	0.32	1.00	1.07	0.48	1.76	0.95	0.90	1.00	0.90	1.35	0.98	0.89
Creep_A	0.33	1.00	1.05	0.47	1.69	0.93	0.82	1.00	0.82	1.37	0.99	0.90
SIM 14o5	0.37	1.00	1.07	0.48	1.68	0.95	0.78	1.00	0.88	1.52	1.07	0.81
SIM 21o5	0.38	1.00	1.06	0.48	1.66	0.94	0.77	1.00	0.87	1.53	1.05	0.82
SIM 23d5	0.36	1.00	1.07	0.48	1.68	0.95	0.81	1.00	0.88	1.50	1.08	0.83
SIM 23o5	0.36	1.00	1.07	0.48	1.68	0.95	0.78	1.00	0.88	1.48	1.08	0.82
SN007a	0.35	1.00	1.08	0.46	1.70	0.95	0.81	1.00	0.90	1.44	1.12	0.84
SN032a	0.33	1.00	1.02	0.45	1.58	0.91	0.81	1.00	0.91	1.48	1.17	0.85

As mentioned previously, the variation between mean values was minimal. The standard deviations were calculated for measurements of mean peak values for all Kevlar

specimens. These values are tabulated in Table 4-4 and 4-5 for the 647 nm incident laser. The standard deviation range for the 1613 cm^{-1} band of FWHM values was 0.0173 to 0.0955. The standard deviation range for the 1613 cm^{-1} band of intensity values was 0.0148 to 0.1000. It should be noted that all standard deviations using the 1064 nm incident laser were much less than the 647 nm deviations.

Table 4-4. Standard deviations for FWHM ratios of all Kevlar specimens.

FWHM Standard Deviations (647 nm laser)							
	Raman Bands (cm^{-1})						
Raman Bands	**# of Tests**	**1187**	**1278**	**1329**	**1518**	**1613**	**1651**
TRI Virgin Strands	**4**	0.1712	0.0000	0.0375	0.4317	0.0267	0.1274
TRI Virgin Yarn	**2**	0.0152	0.0000	0.0993	0.0161	0.0347	0.0654
Virgin Creep	**5**	0.1315	0.0000	0.0672	0.2029	0.0534	0.0844
ATK	**4**	0.0815	0.0000	0.0917	0.3057	0.0848	0.0979
Creep_A	**10**	0.0537	0.0000	0.0621	0.2419	0.0512	0.0847
SIM 14o5	**3**	0.0905	0.0000	0.0058	0.1297	0.0850	0.0543
SIM 21o5	**3**	0.0934	0.0000	0.0654	0.0880	0.0271	0.0615
SIM 23d5	**3**	0.2028	0.0000	0.0225	0.4169	0.0173	0.0325
SIM 23o5	**3**	0.0321	0.0000	0.0918	0.2064	0.0955	0.0499
SN007a	**5**	0.0795	0.0000	0.0410	0.2491	0.0370	0.0222
SN007b	**6**	0.0633	0.0000	0.0663	0.2345	0.0300	0.0265
SN032a	**18**	0.1068	0.0000	0.0904	0.2422	0.0216	0.0288
SN032b	**18**	0.0852	0.0000	0.0960	0.2195	0.0406	0.0353

Table 4-5. Standard deviations for intensity ratios of all Kevlar specimens using a 647 nm incident laser.

Intensity Standard Deviations (647 nm laser)							
	Raman Bands (cm^{-1})						
Raman Bands	**# of Tests**	**1187**	**1278**	**1329**	**1518**	**1613**	**1651**
TRI Virgin Strands	**4**	0.0527	0.0000	0.0333	0.0547	0.0672	0.0559
TRI Virgin Yarn	**2**	0.0037	0.0000	0.0171	0.0128	0.0262	0.0408
Virgin Creep	**5**	0.0269	0.0000	0.0395	0.0274	0.0947	0.0455
ATK	**4**	0.0549	0.0000	0.0458	0.0565	0.0642	0.0291
Creep_A	**10**	0.0341	0.0000	0.0305	0.0265	0.1075	0.0572
SIM 14o5	**3**	0.0670	0.0000	0.0134	0.0106	0.0857	0.0417
SIM 21o5	**3**	0.0291	0.0000	0.0148	0.1146	0.0243	0.0368
SIM 23d5	**3**	0.0269	0.0000	0.0317	0.0631	0.1000	0.0454
SIM 23o5	**3**	0.0436	0.0000	0.0355	0.0605	0.0148	0.0291
SN007a	**5**	0.0187	0.0000	0.0325	0.0265	0.0396	0.0227
SN007b	**6**	0.0113	0.0000	0.0473	0.0303	0.0414	0.0246
SN032a	**18**	0.0260	0.0000	0.0305	0.0398	0.0363	0.0230
SN032b	**18**	0.0230	0.0000	0.0562	0.0418	0.0785	0.0276

From Figure 4-11 the mean values are plotted with the ranges of the 1613 cm^{-1} data using a 647 nm incident laser. The mean values are calculated from 3 to 5 measurements, and the range is the highest and lowest single measurement for that specific specimen. The figure shows how the 1613 cm^{-1} peak becomes broader and less intense for the aged specimen compared to the virgin strands. The lowest FWHM value for the fleet leader specimen was higher than the highest virgin strand value. The lowest intensity value for the virgin strands was higher than the highest intensity value of the SIM specimen.

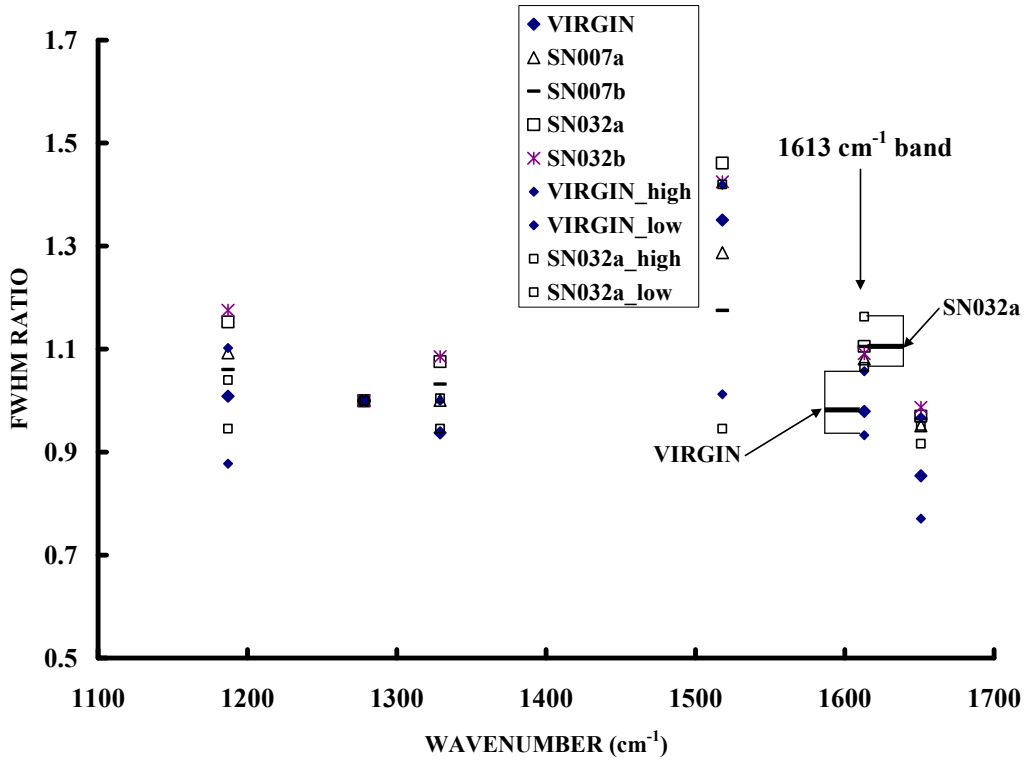

(a)

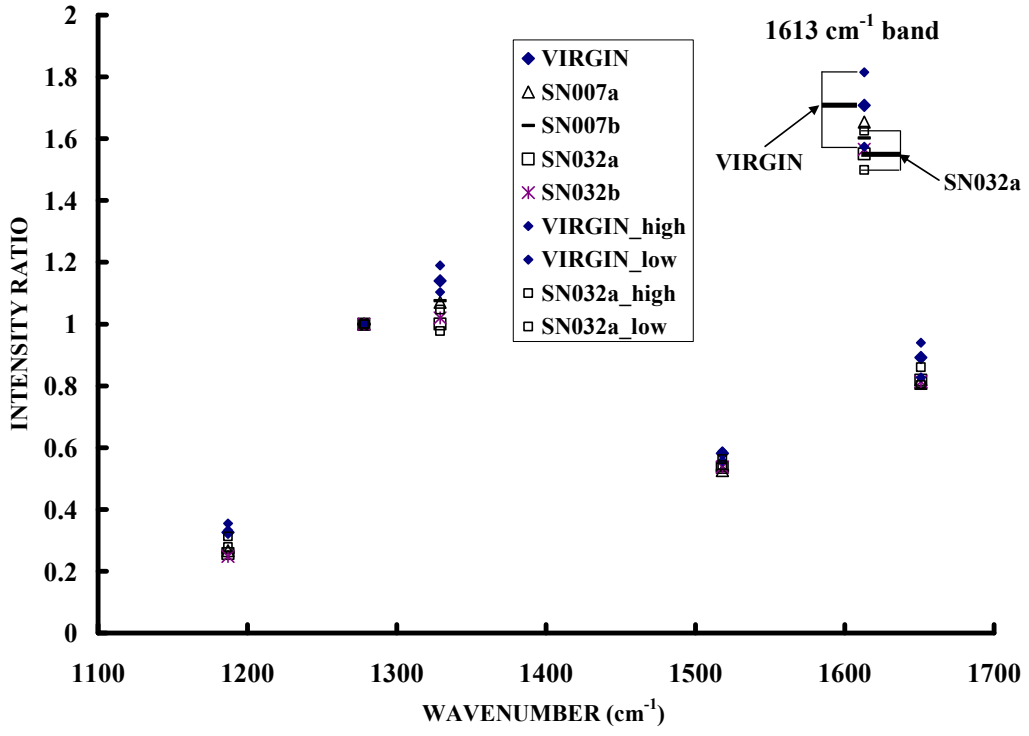

(b)

Figure 4-12. Average values compared with the range for (a) FWHM ratios and (b) intensity ratios of fleet leader specimens.

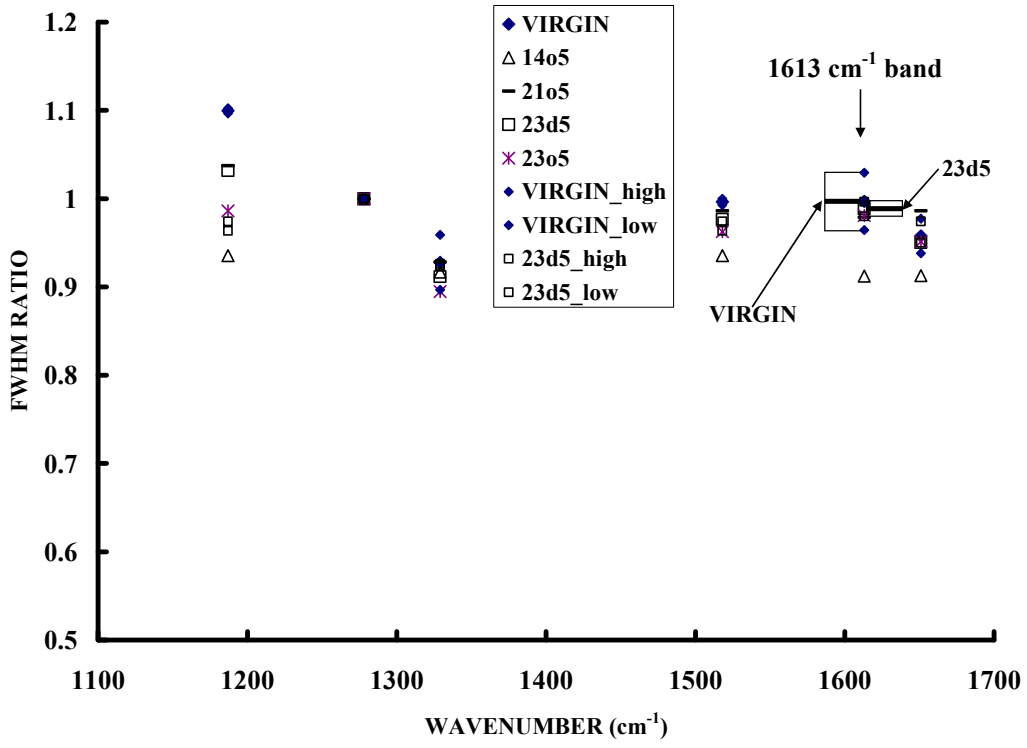

(a)

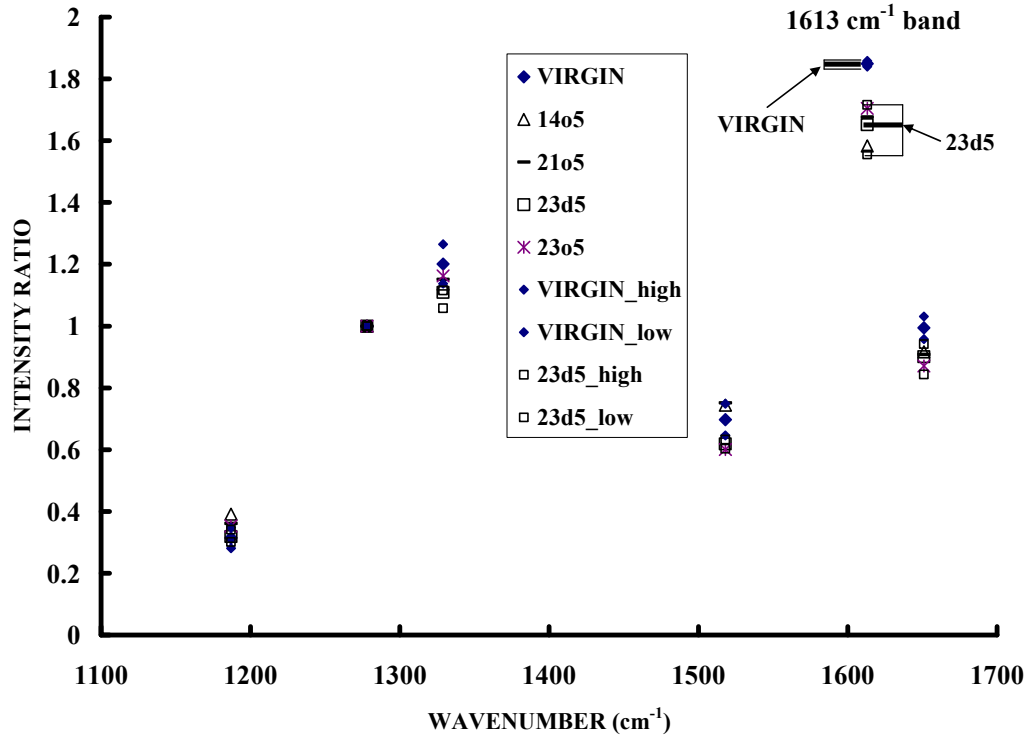

(b)

Figure 4-13. Average values compared with the range for (a) FWHM ratios and (b) intensity ratios of SIM specimens.

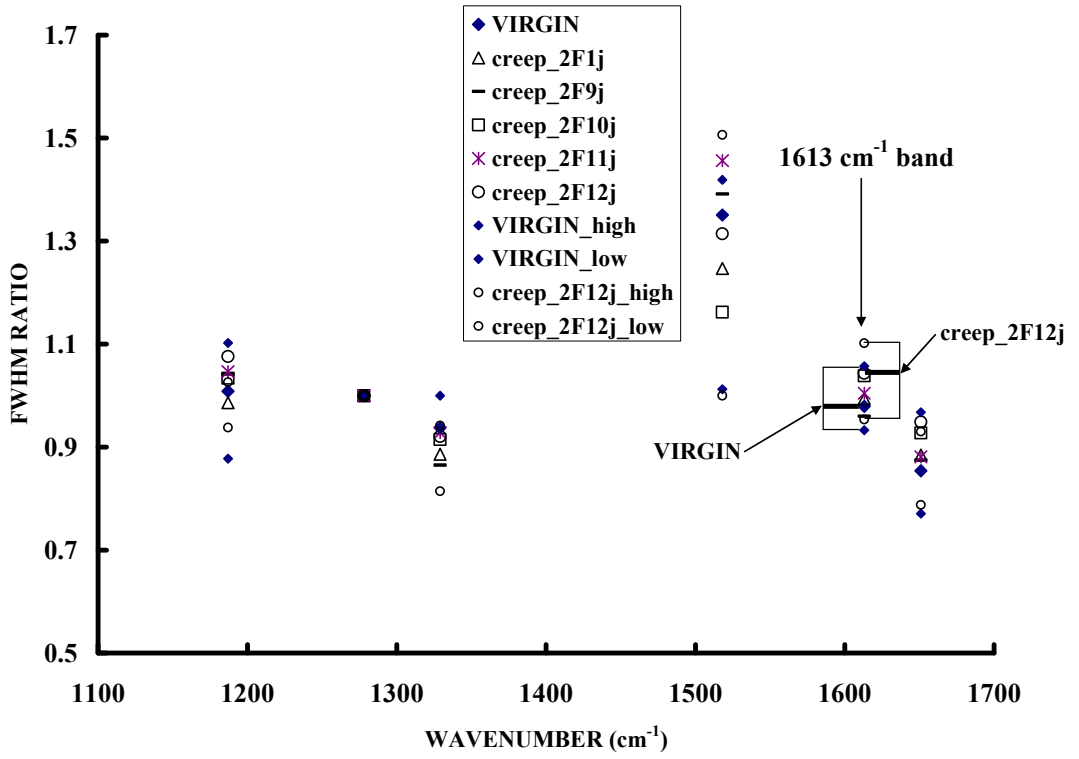

(a)

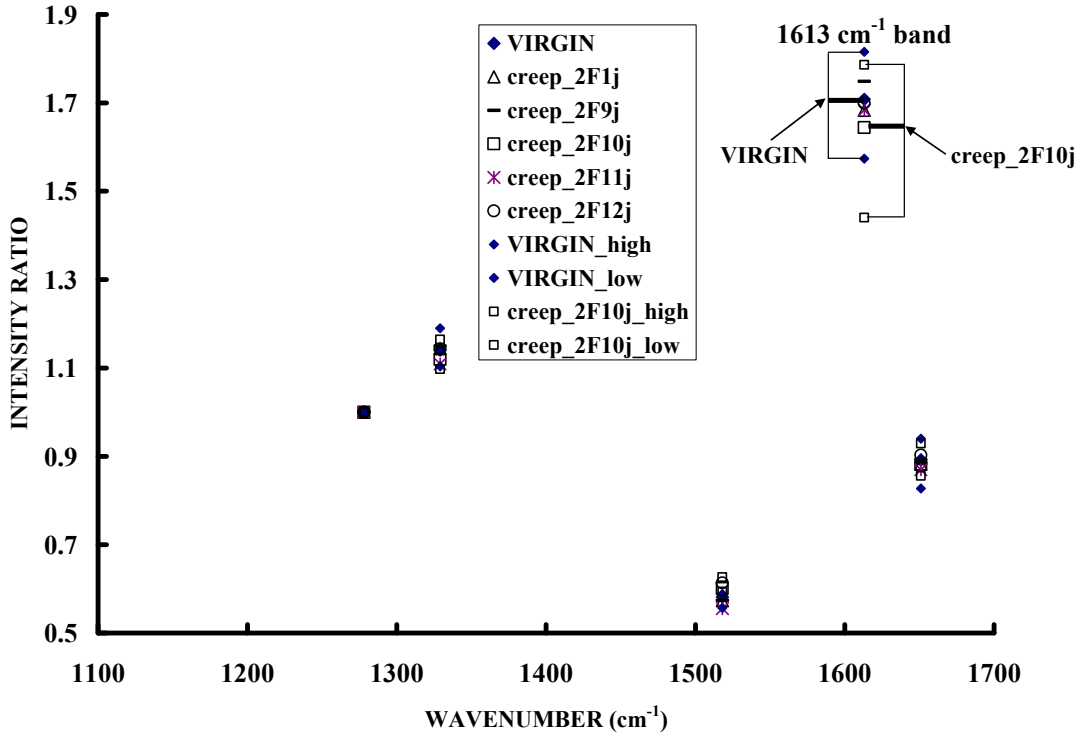

(b)

Figure 4-14. Average values compared with the range for (a) FWHM ratios and (b) intensity ratios of creep specimens.

4.8. Discussion

The goal of this study was to investigate the potential application of Raman spectroscopy as a nondestructive evaluation tool for the detection of aging effects of in-service composite materials. This has been addressed by examining empirically the effects of aging at increased temperature and increased stress on the Raman spectra of Kevlar strands and composite materials. Testing parameters were investigated to develop a firm foundation for evaluating the Raman spectra of Kevlar composites. The testing parameters that effect the empirical relationships of the spectra were laser power, wavelength of incident laser, fiber alignment and fiber focus. These parameters must remain constant for comparing spectra.

It has been observed that aged strand materials from fleet leader, SIM and creep specimens have decreased normalized intensity ratios (η_i) for the 1613 cm^{-1} band when compared to unaged, virgin specimens. It has also been observed that the FWHM ratios (χ_i) have increased for the fleet leader and creep specimens when compared with virgin strand specimens. In other words, the peaks are generally broader and of lower intensity than for virgin, undamaged specimens. Increases in FWHM may be attributed to defects in the fiber or defects being created in the fiber under stress [19]. On a molecular level, rod-like crystallites within the Kevlar distribute loading through hydrogen bonds between adjacent crystallites. Damage to crystallites due to aging phenomena may result in a redistribution of stresses on a molecular level, as damaged crystallites shed loading. On a macroscopic scale, when fiber failure occurs, the load carried from that fiber may be redistributed to adjacent fibers, resulting in a similar effect. When damage occurs such that stresses are variant within the materials, some portion of light may be scattered over

a slightly broader spectrum. For example, the 1613 cm^{-1} band may become broader due to some photons being scattered at the ~1610 cm^{-1} and the ~1618 cm^{-1} regions.

In a study by Stuart, the relative intensities of the major Raman modes were shown to be effected by moisture absorption [18]. From his experiment, a decrease in intensity of the 1613 cm^{-1} band was observed using a FT setup with a 1064 nm incident laser. The decrease in intensity was thought to result from water clusters disrupting the weak hydrogen bonding between crystallites. The decrease in intensity from experimentation reported here may be caused from disruption of hydrogen bonding by extreme temperatures and/or intense loading for the creep, fleet leader, and SIM samples.

It was also observed that peak position was invariant as a result of exposure to increased stress and temperature. This is significant in that there is substantial literature to suggest that peak shifting as a result of applied strain can be used experimentally to determine loading of Kevlar fibers [1, 16, 19]. The observation that these peak positions are unaffected by this "aging" suggests that the relationship between peak position and applied strain could be applied without regard to the "age" of the material. Therefore, evaluation of peak position could form one component of an NDE technique that compared the applied loads in-situ with loading estimated by theoretical models, to locate areas of stress concentration or to analyze the effects of creep.

5

CONCLUSIONS/FUTURE WORK

5.1. Conclusions

Initial experiments have indicated that the Raman spectra of Kevlar can be obtained using a broad spectrum of wavelengths. Variations in peak position resulting from aging have not yet been found. FWHM measurements and intensity measurements using a long wavelength 1064 nm FT Raman system and a 647 nm Renishaw system have shown potential to be utilized for NDE technologies.

Raman spectra can be measured at wavelengths ranging from 488 nm to 1064nm for Kevlar 49. Increased fluorescence was observed at the 488 nm laser line. From data analysis, conclusions are as follows:

- Peak shifts in the Raman spectra resulting from aging were not observed
- Raman bands demonstrated an increase of full width at half maxima (FWHM) ratios for the creep and fleet leader samples compared to the virgin strands
- Raman spectra revealed a decrease in intensity ratios for creep, fleet leader, and SIM samples compared to the virgin strands

It is proposed that these changes in the Raman spectra may be from the disruption of hydrogen bonding between crystallites from aging the Kevlar strands and redistribution of loads within the material, both of which creating a slight change in position of the molecules.

5.2. Future Work

The results of this study indicate that there is potential for the development of NDE technologies based on Raman spectroscopy for the detection of stress rupture for Kevlar COPVs. It should be stressed that the testing conducted to date is limited and exploratory in nature, and further research would be required to develop this technology and further support and investigate the findings reported here.

It should be noted that peak shifting due to aging and stress rupture phenomena was not found during this testing; indicating that strain measurements made via peak shift analysis would not be influenced by material damage i.e. aging. Performing Raman testing on aging materials and analyzing spectrum for peak shifting, intensity changes and FWHM increases may provide a foundation for condition assessment of the material, and has the potential to be developed as an NDE technology.

Another recommended approach to detect the onset of stress rupture would involve in-situ testing using Raman spectroscopy using a fiber optic microprobe. Fiber optic probes are available that attach to the Renishaw Raman systems which would allow for testing in the field. The flexible fiber optics allows the microprobe to operate in the horizontal, vertical and multi-angle positions [23]. For example, if a composite over-

wrapped pressure vessel was pressurized in service, Raman measurements can be obtained, and the spectra could then be examined for peak shifts. If the peak shifts are too great, the vessels may be susceptible to failure due to stress rupture. This data could also be analyzed for FWHM and intensity Raman band values for the detection of "aging" effects of Kevlar composite materials. Further investigation is needed to study this phenomenon in the field.

REFERENCES

1. Schadler, L.S., Galiotis, C., *Fundamentals and Applications of Micro Raman Spectroscopy to Strain Measurements in Fiber Reinforced Composites.* International Materials Reviews, 1995. **40**(3): p. 116-133.
2. Gerstle, F.P. *Prediction of Long-term Failure in Kevlar 49 Composites*. in *SAND-81-2072C; CONF-820340-2*. 1982. Sandia National Laboratories - Albuquerque, NM.
3. Washer, G., Allempalli, S. *NDE Technologies for Condition Assessment of FRP Retrofits*. in *ASNT Fall Conference*. 2005. Columbus, OH.
4. Karbhari, V.M., Chin, J.W., Hunston, D., Benmokrane, B., Juska, T., Morgan, R., Lesko, J.J., Sorathia, U., Reynaud, D., *Durability Gap Analysis for Fiber-Reinforced Polymer Composites in Civil Infrastructure.* Journal of Composites for Construction, 2003(August): p. 238-247.
5. Yang, H.H., *Kevlar Aramid Fiber*. 1993, New York: Wiley.
6. Kumar, B.G., Singh, R. P., Nakamura, T., *Degradation of Carbon Fiber-reinforced Epoxy Composites by Ultraviolet Radiation and Condensation.* Journal of Composite Materials, 2002. **36**(24).
7. Zeifman, M.I., Ingman, D., *Statistical Aspects of Lifetime in the Presence of UV Radiation.* Journal of Electronic Packaging, 2003. **125**(1): p. 1-3.
8. Mahesh, S., Phoenix, S. L., *Lifetime distributions for unidirectional fibrous composites under creep-rupture loading.* International Journal of Fracture, 2004. **127**: p. 303-360.
9. Otani, H., Phoenix, S. L., Petrina, P., *Matrix Effects on Lifetime Statistics for Carbon-Epoxy Microcomposites in Creep Rupture.* Journal of Materials Science, 1991. **26**: p. 1955-1970.
10. Koenig, J.L., *Spectroscopy of Polymers*. Koenig, J.L. 1992, Washington, DC: ACS Professional Reference Book.
11. Amer, M.S., Schadler, L.S., *The Effect of Interphase Toughness on fibre/Fibre Interaction in Graphite/Epoxy composites: An Experimental and Modelling Study.* Raman Spectroscopy, 1999. **30**: p. 919-928.
12. Penn, L., Milanovich, F., *Raman Spectroscopy of Kevlar 49 Fiber.* Polymer, 1979. **20**(1): p. 31-36.
13. Kim, P.K., Chang, C., Hsu, S.L., *Normal Vibrational Analysis of a Rigid Rod Polymer: poly(p-phenylene terephthalamide).* Polymer, 1986. **27**(1): p. 34-46.
14. Chang, C., Hsu, S. L., *An Analysis of Strain-Induced Frequency Changes in Poly (p-phenylene terephthalamide) Single Fibers.* Macromolecules, 1990. **23**: p. 1484-1486.
15. Andrews, M.C., Bannister, D.J., Young, R.J., *The Interfacial Properties of Aramid/Epoxy Model Composites.* Journal of Materials Science, 1996. **31**: p. 3893-3913.
16. Galiotis, C., Robinson, I.M., Young, R.J., Smith, B., Batchelder, D. N., *Strain Dependence of the Raman Frequencies of a Kevlar 49 Fiber.* Polymer Communications, 1985. **26**: p. 354-355.

17. Kawagoe, M., Hashimoto, S., Nomiya, M., Morita, M., Qiu, J., Mizuno, W., Kitano, H., *Effect of Water Absorption and Desorption on the Inerfacial Degradation in a Model Composite of an Aramid Fiber and Unsaturated Polyester Evaluated by Raman and FT Infra-red Microscopy.* Journal of Raman Spectroscopy, 1999. **30**: p. 913-918.
18. Stuart, B.H., *A Fourier Transform Raman Study of Water Sorption by Kevlar-49.* Polymer Bulletin, 1995. **35**: p. 727-733.
19. Prasad, K., Grubb, D.T., *Deformation Behavior of Kevlar Fibers Studied by Raman Spectroscopy.* Journal of Applied Polymer Science, 1990. **41**: p. 2189-2198.
20. Ding, H., Varlow, B. R., *Raman Spectroscopy-A Technique to Assess the Residual Stress in Fiber-Reinforced Polymeric Insulation Materials*, in *IEEE Electrical Insulation Magazine*. 2004. p. 5-13.
21. Alwis, K.G.N.C., Burgoyne, C. J. *Stepped Isothermal Method for Creep Rupture Studies of Aramid Fibers*. in *ACI Special Publications*. 2005.
22. Galiotis, C., Robinson, I.M., Young, R.J., Batchelder, D. N., ed. *Strain Measurements in Aramid Fibers and Composites Using Raman Spectroscopy*. Engineering Applications of New Composites. 1988.
23. Parthenios, J., Katerelos, D. G., Psarras, G.C., Galiotis, C., *Aramid fibers; a multifunctional sensor for monitoring stress/strain fields and damage development in composite materials.* Engineering Fracture Mechanics, 2002. **69**: p. 1067-1087.
24. Young, R.J., Day, R.J., Lu, D., *Raman Spectroscopy of Kevlar Fibers during Deformation - Caveat Emptor.* Polymer International, 1991. **24**: p. 71-76.